Swiss J Palaeontol (2013) 132:23–44
DOI 10.1007/s13358-012-0050-y

Taphonomy and palaeoecology of the green Devonian gypidulid brachiopods from the Aferdou El Mrakib, eastern Anti-Atlas, Morocco

Lorena Tessitore · Mena Schemm-Gregory · Dieter Korn · Ferdinand R. W. P. Wild · Carole Naglik · Christian Klug

Received: 27 August 2012 / Accepted: 11 December 2012 / Published online: 12 February 2013

Abstract On Aferdou El Mrakib, a large reef mound in the Maïder region (Anti-Atlas, Morocco), thick-shelled gypidulids of two genera are locally very abundant. Like *Stringocephalus* in the shallow water limestone formations in Germany, these Moroccan brachiopods of the genera *Devonogypa* and *Ivdelinia* often display greenish shells. By analysing these shells by EDX, it turned out that the colour was possibly caused by impurities of Fe^{2+}-ions. The concentration varies, indicating that the colour is less dependent on the concentration than on shell thickness, because only the thickest parts of the shells appear green and thin-shelled forms never display the green colour. There is also some indication that the Fe content increases towards deeper shell layers (further away from the surface). In addition, we examined the quality and spatial distribution of sublethal injuries in over 200 specimens of *Devonogypa* and *Ivdelinia*. Shape, spatial distribution on the shells, and abundance of the sublethal injuries support the hypotheses that (1) the injuries had several causes, (2) some of these were inflicted by predators, probably cephalopods, and (3) many fractures and deformations might have been caused by the brachiopod shells hitting each other in dense populations in agitated water. The existence of dense clusters, built by the association of members of both genera or of only one taxon, is corroborated by the patchy occurrence of these brachiopods.

Keywords Brachiopods · Taphonomy · Palaeoecology · Reef-mounds · Devonian · Morocco

Electronic supplementary material The online version of this article (doi:10.1007/s13358-012-0050-y) contains supplementary material, which is available to authorized users.

L. Tessitore (✉) · C. Naglik · C. Klug
Palaeontological Institute and Museum, University of Zurich, Karl Schmid-Strasse 4, 8006 Zurich, Switzerland
e-mail: lorena.tessitore@uzh.ch

C. Naglik
e-mail: carole.naglik@pim.uzh.ch

C. Klug
e-mail: chklug@pim.uzh.ch

M. Schemm-Gregory
Centro de Geociências da Universidade de Coimbra, Largo Marquês de Pombal, 3000-272 Coimbra, Portugal
e-mail: Mena.Schemm-Gregory@dct.uc.pt; Mena.Schemm@gmx.de

D. Korn
Museum für Naturkunde, Leibniz-Institut für Evolutions- und Biodiversitätsforschung, Humboldt-Universität, Invalidenstraße 43, 10115 Berlin, Germany
e-mail: dieter.korn@mfn-berlin.de

F. R. W. P. Wild
Anorganisch-chemisches Institut, University of Zurich, Winterthurerstrasse 190, 5087 Zurich, Switzerland
e-mail: fwild@aci.uzh.ch

Introduction

The Devonian succession of sedimentary rocks in Morocco has become famous in the past century mainly for its richness in fossils but also for its remarkably well-exposed carbonate build-ups (e.g., Roch 1934; Massa et al. 1965; Hollard 1974; Töneböhn 1991; Brachert et al. 1992; Wendt 1993; Belka 1994, 1998; Kaufmann 1997, 1998; Kaufmann et al. 1999; Bultynck and Walliser 2000; Aitken et al. 2002; Cavalazzi et al. 2007; Berkowski and Klug 2012). One of these, Aferdou El Mrakib, is a conspicuous structure in the Maïder region in the eastern Anti-Atlas, about 70 km SW of Rissani (Fig. 1). It is a reef mound of early Givetian age, which measures ca. 900 m in diameter and ca. 100–130 m in elevation above the underlying strata and hence is the

largest carbonate build-up in the Maïder Basin (Wendt 1993; Kaufmann 1996, 1997, 1998). Its geometry is almost circular in outline with a truncated cone-shape (Kaufmann 1997, 1998).

This reef mound contains the most diverse fauna among the carbonate build-ups in the Maïder (Kaufmann 1998). In addition to the usual Devonian reef fauna, the two large gypidulid brachiopods *Ivdelinia pulchra* Franchi et al.

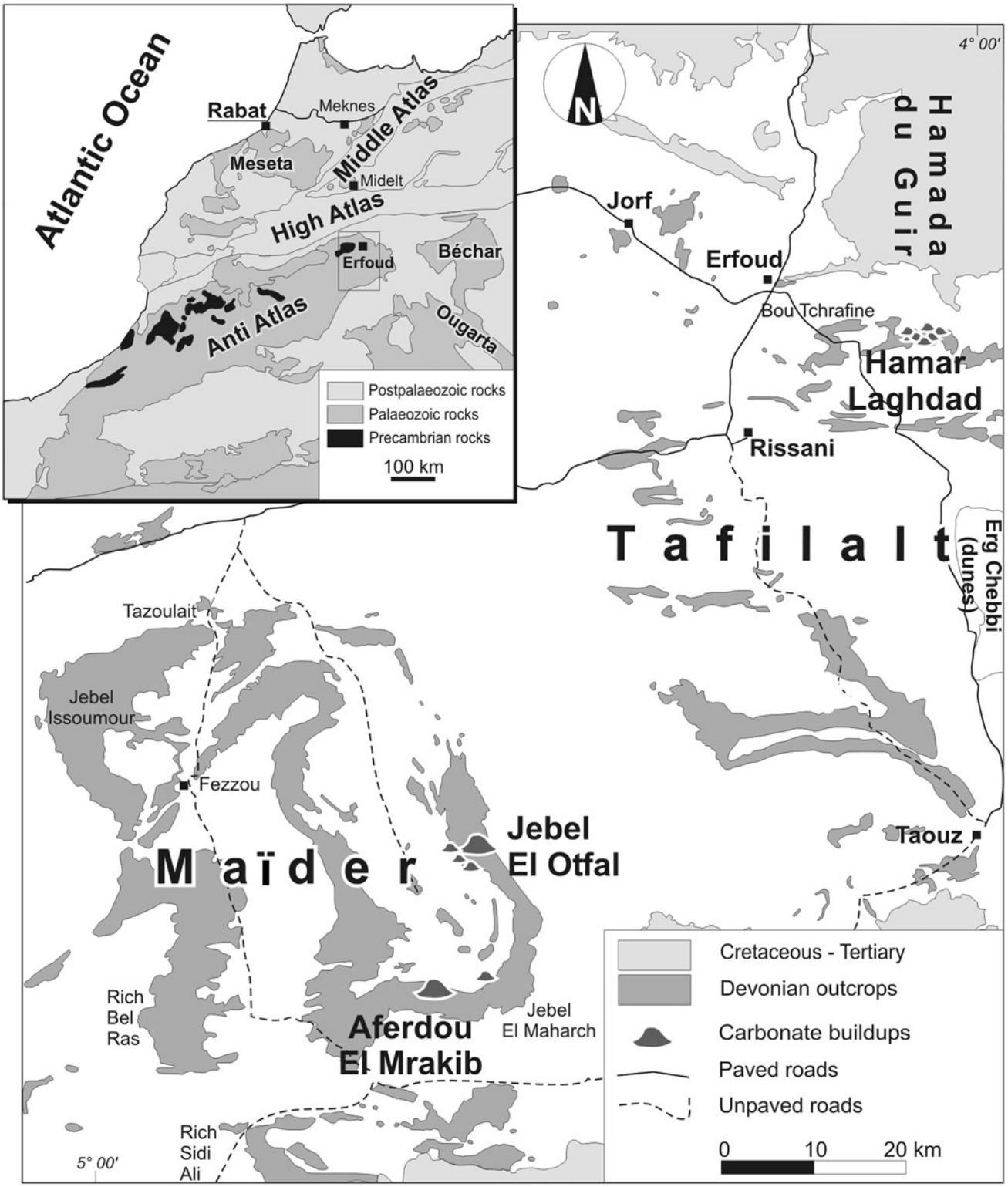

Fig. 1 Map showing the localisation of the reef mound Aferdou El Mrakib and other carbonate build-ups in the Maïder (modified after Klug 2002)

(2012) and *Devonogypa* sp. are particularly abundant in the sediments of this mountain (Fig. 2). Their greenish shell colour and patchy mass occurrences have already attracted the attention of some palaeontologists (e.g., Franchi et al. 2012; Z. Belka, Posnan, and A. T. Halamski, Warszawa are currently preparing comprehensive papers on Aferdou El Mrakib and its brachiopod fauna).

Although mentioned by Kaufmann (1998), the mass occurrences of the two rather large gypidulids *Ivdelinia pulchra* (40 × 45 mm) and *Devonogypa* sp. (70 × 77 mm) had not been studied in detail until recently. In a first study, Franchi et al. (2012) described a new species of *Ivdelinia* based on material from the Aferdou El Mrakib. In addition, the entire brachiopod fauna of this reef mound is still a present work subject of different authors. It will also be the subject of a project, which has much broader scope, dealing with several sedimentological and palaeontological aspects of this prominent geological feature. Nevertheless, the peculiar taphonomy of these thick-shelled brachiopods, especially the origin of the green colour of their shells, has not been assessed before (compare Klug et al. 2009). In addition, palaeoecological aspects of these mass occurrences of gypidulids were also never examined in detail. In this study, we discuss the injuries that left traces in most of the shells we have collected. Sublethal injuries and other shell deformities in brachiopods have repeatedly been described by various authors (some Palaeozoic examples: Brunton 1966; Elliott and Bounds 1987; Elliott and Brew 1988; Bordeaux and Brett 1990; Brett and Walker 2002; Balinski 1993; Balinski and Biernat 2003). As in molluscs, it is difficult to find evidence for the cause of these injuries, which are also discussed.

Therefore, the aims of this study were (1) to examine the preservation of these large, thick-shelled gypidulid brachiopods, and (2) to document and evaluate, both statistically and qualitatively, the sublethal injuries found in these brachiopods. These results might help to answer the question whether their mass occurrences are caused by taphonomic shell accumulations or whether they represent more or less autochthonous accumulations of the two species.

Material

The material contains specimens belonging mainly to the two brachiopods *Ivdelinia pulchra* (Fig. 3) and *Devonogypa* sp. (Fig. 4), which attained large sizes on the reef mound Aferdou El Mrakib. In addition, the accompanying fauna was sampled, which is present throughout the mound and which contains various species of other brachiopods, trilobites (in association with the gypidulids, phacopids and scutellids are the most common groups), crinoids, gastropods, corals, stromatopores, bryozoans, and cephalopods.

In order to draw conclusions on the taphonomy of these two gypidulids, we also examined the thick-shelled brachiopod *Stringocephalus* from Germany, which apparently underwent a similar kind of taphonomy (as reflected in local occurrence of greenish shells) and which had habitat preferences similar to those of *Ivdelinia* and *Devonogypa*, i.e. shallow, agitated water and a reef or reef-like environment.

Institutional abbreviation—PIMUZ, Paläontologisches Institut und Museum, University of Zurich, Switzerland (PIMUZ 30018–30213, PIMUZ 30214–30218).

Methods

Geochemical analyses of the shells of *Ivdelinia pulchra* and *Devonogypa* sp. from Aferdou El Mrakib (Morocco) and of *Stringocephalus* sp. from Warstein (Germany) were performed (Tables 1, 2, online material) with a Jeol JSM-6060 scanning electron microscope (SEM) equipped with Bruker Quantax EDX detector, having an energy resolution of 126 eV in the Institute of Inorganic Chemistry of the University of Zurich. Element concentrations were determined with the help of the Bruker Esprit 2.1 software. The principles of the "standard free" determination of elements by EDX are described in Eggert (2005). For preservation of the samples, these were not coated but wrapped in aluminium foil exhibiting small windows for the measurements. In addition, braided copper wires grounded the samples, preventing static electricity build-up. The concentration of the elements Cu and Al may be biased by the fact that they were used as foils wrapped around the samples to make them sufficiently conductive for the SEM analysis. The findings for both elements are not discussed for this reason.

Many of the brachiopod shells display injuries. Remarkably, the majority of injuries were found on the ventral valve (an exception is visible in Fig. 4: 1d, e, on the right). We think that this might have been caused partially by the fact that the ventral valve has a much larger surface area and by the fact that the dorsal valve pointed more or less upward syn vivo and was thus more protected. In order to enhance contrasts and make the injuries better visible, the ventral valves of all specimens were first whitened by NH_4Cl and then photographed approximately in the same position. Second, these images and the actual specimens were examined for healed injuries. Third, the angular distance of all injuries from the plane of symmetry of the specimens was measured (Fig. 5; Table 2). We measured the angle with a thin plastic foil, which displays lines arranged radially, separated by an angle of 10° each. This sheet was wrapped around the injured specimens to measure the angular distance of the injuries from the plane


a
b
c
d
e
f
g

◀ **Fig. 2** Gypidulid brachiopod-occurrences on Aferdou El Mrakib, Maïder, Morocco. **a** Freshly broken rock with *Ivdelinia pulchra* (*left*) and *Devonogypa* sp. (*top*, *centre*); note the *green colour*; all specimens preserved with both valves, i.e. an autochthonous to parautochthonous occurrence; *pocket knife* for scale (length 9 cm); **b** > 1 m thick limestone layer composed mostly of *Ivdelinia pulchra*; *hammer* for scale (length 30 cm); **c** layer with large *Devonogypa* sp. with thick internal cement crusts; note the *greenish shell colour*; *pocket knife* for scale; **d** ca. 1 m thick lense with *Ivdelinia pulchra*, which occurs in rockforming numbers; *hammer* for scale (length 30 cm); **e** *Devonogypa* sp., weathered out of the mound-limestones; **f** ca. 30 cm thick limestone with many isolated allochthonous gypidulid shells

of symmetry. The point where all the lines meet was put on the umbo with the lines diverging away from the umbo. We used this foil because if the angle is measured from a photo in 2D, this causes an artificial accumulation of injuries, where the shell is strongly vaulted. In addition, on images, not all injuries are easily detectable.

The injuries were also classified according to their size and shape. We distinguished several different kinds of injuries; they vary between less than 1 mm to several centimetres in size (Fig. 6):

Type 1 Long radial furrows, which may occur on the entire shell;
Type 2 A single hole;
Type 3 Two symmetrical subcircular convex depressions (like holes or ditches);
Type 4 Two small symmetrical drop-shaped convex depressions (like holes or ditches);
Type 5 Two large symmetrical more or less crescent-shaped depressions;
Type 6 A single hole followed by a radial trace throughout the shell to the commissure;
Type 7 Like type 6, but in form of a nail because of a much broader trace;
Type 8 Symmetrical pair of radial furrows;
Type 9 Transverse shell fractures causing intense deformation/swelling of the subsequent shell;
Type 10 Transverse fracture without consequences for later growth; no mantle injury;
Type 11 Growth irregularities, where growth line spacing and strength vary;
Type 12 Small bulge with a central pit, reminiscent of pearls or Housean pits (De Baets et al. 2011), possibly caused by foreign particles or parasites;

The smallest injuries are the types 2–5, which measure less than 4 mm in diameter. By contrast, the radial traces and transverse shell fractures may reach lengths of 30–40 mm. *Devonogypa* sometimes display very broad ribs, which probably are also caused by injuries early in ontogeny.

There are two possible biases in this analysis: (1) some of the injuries were quite broad; in such cases, we measured at the centre of the injury. It might occur, however, that the injury is not well visible on one side and in such case, the angle might be inaccurate. We consider this error as not very important. (2) At least in *Ivdelinia*, the stronger differentiation between sulcus and fold has some effect by protecting the middle part, reducing the abundance of injuries near the middle by its shape, at least in the ventral valve.

Geological setting

Aferdou El Mrakib is the largest reef mound in the Maïder Basin (Fig. 1). It is of Givetian age (Kaufmann 1996, 1997) and was first described by Hollard (1974) and later again by Wendt (1993). The main kinds of rocks in this carbonate build-up are boundstone, wackestone, packstone, and floatstone. The base of the Givetian is marked by a 2 m thick coral-stromatoporoid boundstone, which directly underlies the reef mound and probably served as a pioneer stage in the mound development (Kaufmann 1998). The sediments of Aferdou El Mrakib consist of crinoidal grainstone, trilobite wackestone, poorly fossiliferous mudstone, brachiopod lenses, and mound debris deposits, sometimes with several metre large olistoliths. Many of these deposits have been affected by erosion. For instance, the lateral transition of the mound debris facies to the coeval off-mound facies is not preserved (Kaufmann 1998).

About 100–130 m of the original height of the reef mound is preserved. Its largest diameter is 900 m, which apparently represents its largest original diameter. Even though remains of large potential frame builders such as *Heliolites* sp. (up to >1 m in diameter; Fig. 7) occur and while these reef organisms are locally abundant on the reef mound, these organisms never formed a true frame on Aferdou El Mrakib (Kaufmann 1998; Franchi et al. 2012), at least not in the preserved part. The mound grew concentrically, expanding both laterally and vertically, but it was also affected by erosion (Kaufmann 1998). Although a valley is deeply incised into the reef mound, it does not exhibit its internal structure entirely and much of the central part is dolomitized. In the dolomitized parts, the fossils, and sedimentary structures were more or less obliterated (Kaufmann 1998), but relics of some larger fossils such as large corals or brachiopods are still visible where dolomitization was less intense. According to Kaufmann (1998), the mound debris facies is only preserved on the northern and western flanks. He also stated that some small-scale fissures and neptunian dykes occur throughout the Aferdou El Mrakib.

The brachiopod lenses described by Kaufmann (1998) are composed mainly of the two large gypidulid genera *Ivdelinia* and *Devonogypa*. As already mentioned by Franchi et al. (2012), the occurrence of these two genera is rather patchy. Sometimes, they occur in single specimens (e.g., in the mound debris facies), sometimes in small clusters of a few to some tens of specimens, and in some places, especially on the northwestern flank of the build-up, they occur in large masses (thousands of specimens) in layers some tens of centimetres up to several metres in thickness (Fig. 2).

In some spots, only one of the two species occurs and sometimes they occur together. The co-occurrences of these two gypidulids (Franchi et al. 2012) show that they shared several palaeoecological requirements to some degree (water depth, elevated habitat, etc.), probably also with *Stringocephalus* (compare, e.g., Boucot et al. 1966; Balinski 1971).

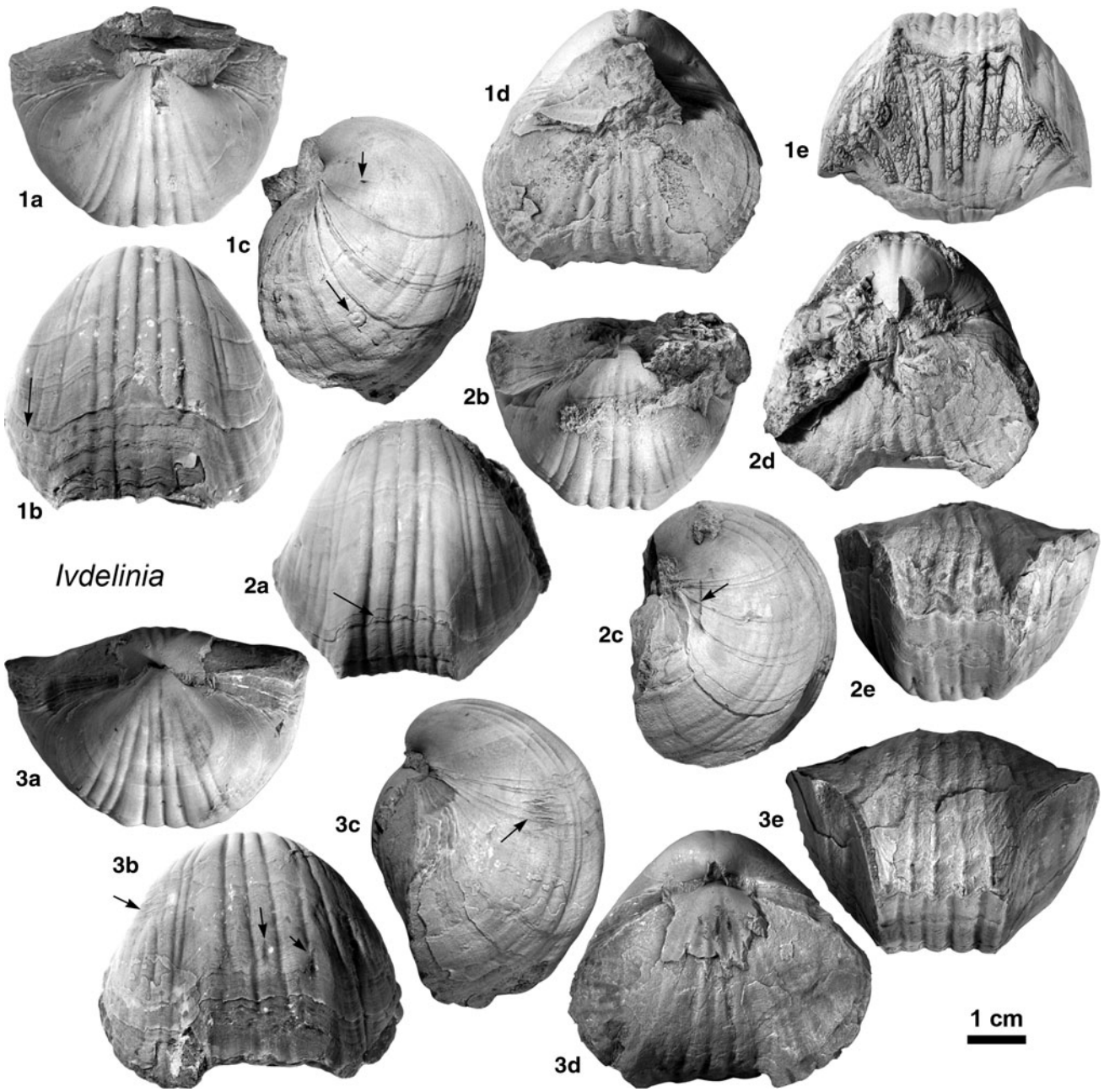

Fig. 3 *Ivdelinia pulchra* from the Givetian mound facies of the northwestern flank of Aferdou El Mrakib, Maïder, Morocco. *Arrows* mark sublethal injuries. All specimens × 1, coated with NH_4Cl. **1** PIMUZ 30037; **2** PIMUZ 30018; **3** PIMUZ 30164

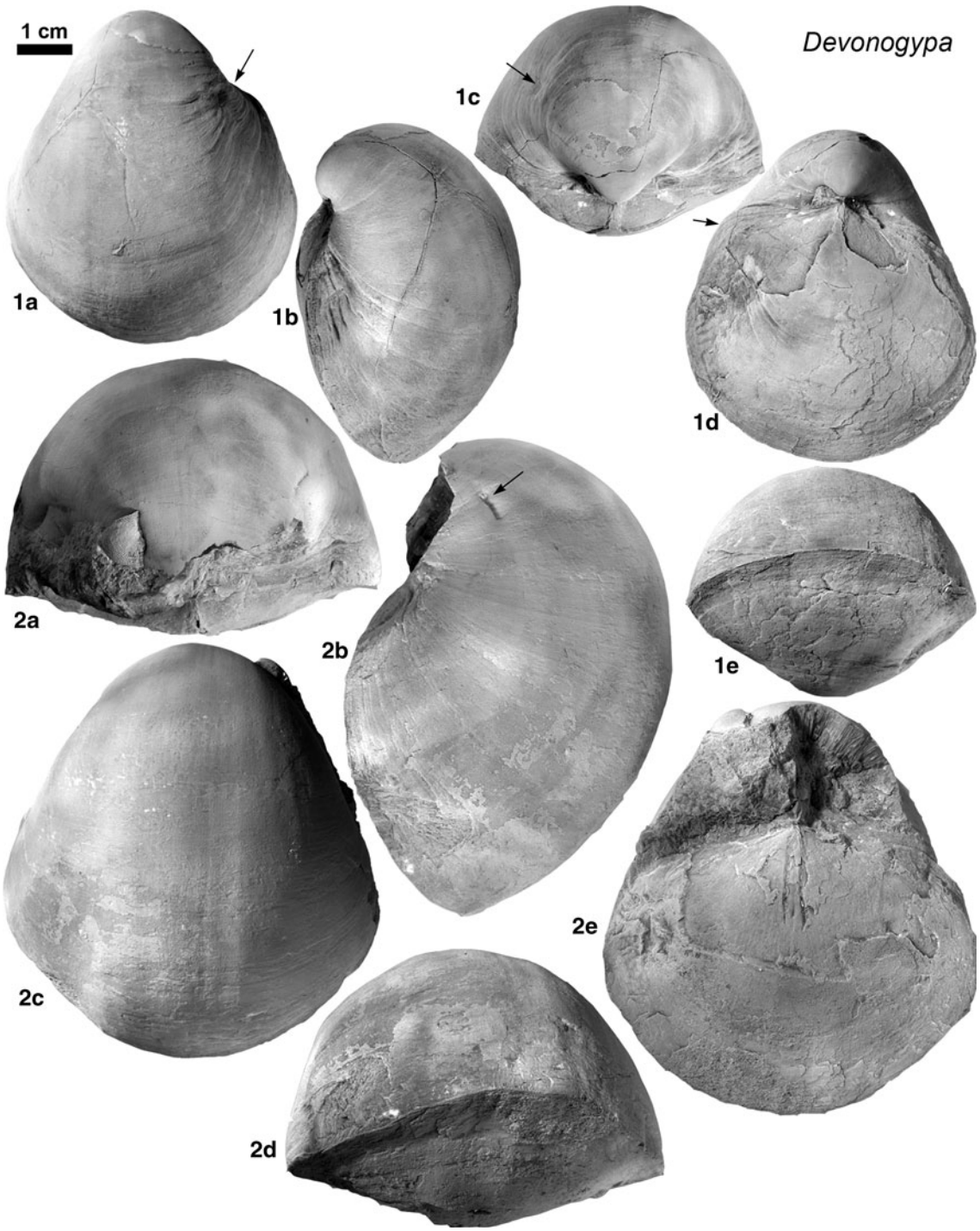

Fig. 4 *Devonogypa* sp. from the Givetian mound facies of the northwestern flank of Aferdou El Mrakib, Maïder, Morocco. *Arrows* mark sublethal injuries. All specimens × 1, coated with NH_4Cl. **1** PIMUZ 30151; **2** PIMUZ 30141

Several other species of brachiopods co-occur with the gypidulids, which are less abundant than the two gypidulids. For instance, the gypidulid mass occurrences rarely contain atrypids, which are very common in the reef debris-facies in the Northeast of Aferdou El Mrakib.

The German material of *Stringocephalus* used for comparison here comes from the abandoned limestone quarry "Warstein Hauptstraße" (51.4488°N, 8.35820°E), where a roughly 80 m thick succession of grey Middle Devonian reef debris limestone (so-called Massenkalk) is exposed.

The outcrop lies near the centre of the Warstein Anticline at the northern margin of the Rhenish Slate Mountains (Rheinisches Schiefergebirge). Reef debris limestones

of Givetian age (Clausen and Leuteritz 1984) are exposed in the axis of the anticline, extending for about 6 km in a WSW–ENE direction. The total thickness of this limestone unit is unclear because its base is not exposed; estimations range between 200 and 300 m (Clausen and Leuteritz 1984). The grey limestone contains remains of stromatoporoids, tabulate and rugose corals, brachiopods (*Stringocephalus*), and occasionally gastropods.

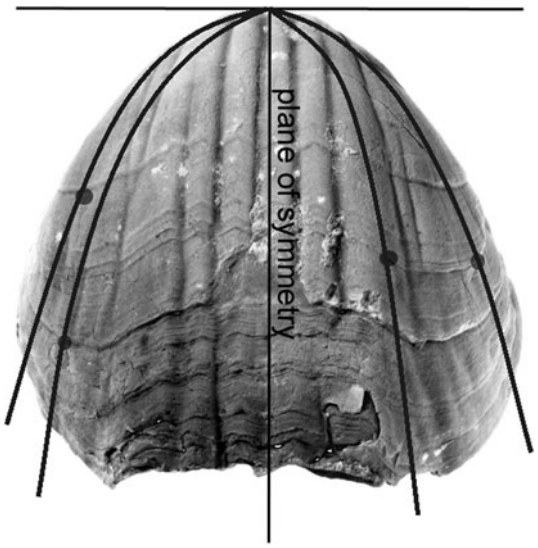

Fig. 5 Measurement of the relative position of sublethal injuries

The entire area of the Warstein Anticline is affected by tectonic deformation, and this is particularly well visible in the *Stringocephalus* Limestone. Deformation led here to a significant elongation of the brachiopod specimens toward ten times of the length parallel to the cleavage (Richter-Bernburg 1953; Clausen and Leuteritz 1984). The shells of the brachiopod specimens are recrystallized into sparry calcite.

Chemical composition of brachiopod shells from the reef mound

In order to understand the origin of the green colour of the gypidulids from the Aferdou El Mrakib reef mound, we measured the element composition of *Devonogypa* sp. and *Ivdelinia pulchra.* For comparison, the element compositions of two additional species were also measured, one being a small rhynchonellid from the Moroccan reef mound, which has a greyish shell colour, and one being *Stringocephalus* sp. from Germany, which is also green, but a slightly darker shade (Fig. 8). With these analyses, it

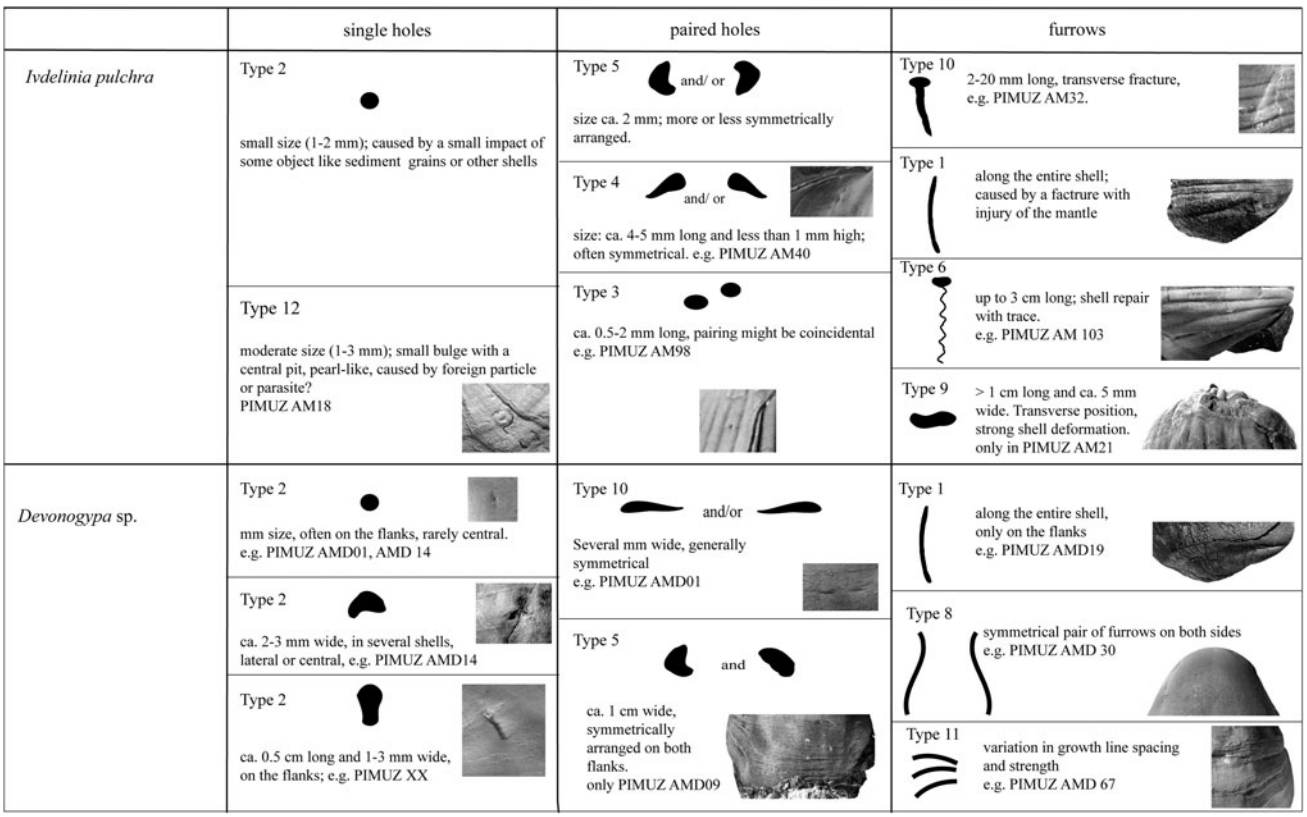

Fig. 6 Types of injuries found in the gypidulids from Aferdou El Mrakib, Morocco

Fig. 7 *Heliolites* sp., Givetian, northwestern flank of Aferdou El Mrakib, Morocco. The entire block is part of one large colony, which probably exceeded one metre in diameter

was possible to find out whether the shell colour is linked to certain taxa (only gypidulids or also in terebratulids and rhynchonellids) and whether the colour depends on the shell thickness of the specimen or not. In the following, we list the results of the EDX-analyses arranged according to the analysed taxa and specimens.

Stringocephalus

The examined specimen of *Stringocephalus* sp. from Germany (PIMUZ 30218) is strongly deformed and has a rather dark greenish shell, although the colour varies significantly within the shell from nearly white to green (Fig. 8c). Within this shell, a high mean concentration of iron was detected (1.87 wt %; Table 1, online material). Analyses revealed that the composition changes from the surface inwards. Indeed, the elements Fe, Ca, K, Cl, S, Si, Mg, and Na show an increase in concentration, while the contents of Mn, Cu, Al, as well as C and O do not show a significant change. Generally, this difference in composition is almost 1 wt. %.

On the surface (PIMUZ 30218; Objects 304, 305, 309, Fig. 8), Fe occurs in amounts as high as 2.16 % (Table 1), while Mn is almost absent. Inwards (Objects 302, 307, 308), the values of Fe increase from values of 2.16 wt % to values of 2.68 wt %. The same was found for the Mn-values, which changed from 0.40 wt % on the surface to 0.55 wt % inside the shell. The clay elements (Al, Cl, K, Si, Ca, O, Fe, Na, Mg, P, S, Mn) increase in their concentration towards the inside by almost 1–2 wt % except Ca, which increases to almost 4 wt %. To the extreme top and bottom of the examined section, the concentrations in Fe and Mn decrease, which is probably linked to the distribution of the greenish shades. On the bottom (Objects 301, 310) of this shell, a pyrite incrustation is observed, where the Fe concentration is much higher.

Devonogypa sp.

Compared to *Stringocephalus*, the shell of the Moroccan *Devonogypa* sp. (PIMUZ 30214; Fig. 8f) has a slightly more yellowish-greenish colour, with a mean Fe concentration (1.1 wt %) being somewhat lower than in *Stringocephalus* (1.87 wt %).

The large specimen of *Devonogypa* sp. (PIMUZ 30214) from Aferdou El Mrakib has been analysed from the surface (greenish colour) towards the inner part, where the colour changes (Fig. 8f). On the surface (Object 1), the analyses indicate a composition rich in clay elements (Ca, O, Cl, K, Na, Si, Fe, Mn, P, S) and in Cu as well as Fe (Table 1). On the surface of the shell, the most abundant elements are Si and Al (Objects 2, 3, 4; Appendix). A little bit below the surface (Objects 10, 11, 12), the Fe increases to 2.1 wt % and the content of Cl follows the rises even if only for 0.07 % from 1.15 to 1.22 wt %. At least in the inner part of the shells (Objects 13, 14, 15; Appendix), Fe and Mn occur in lower amounts and the clay components are still predominant.

Cl is found in all objects and seems to be an important shell-component of *Devonogypa* sp. (PIMUZ 30214). Most

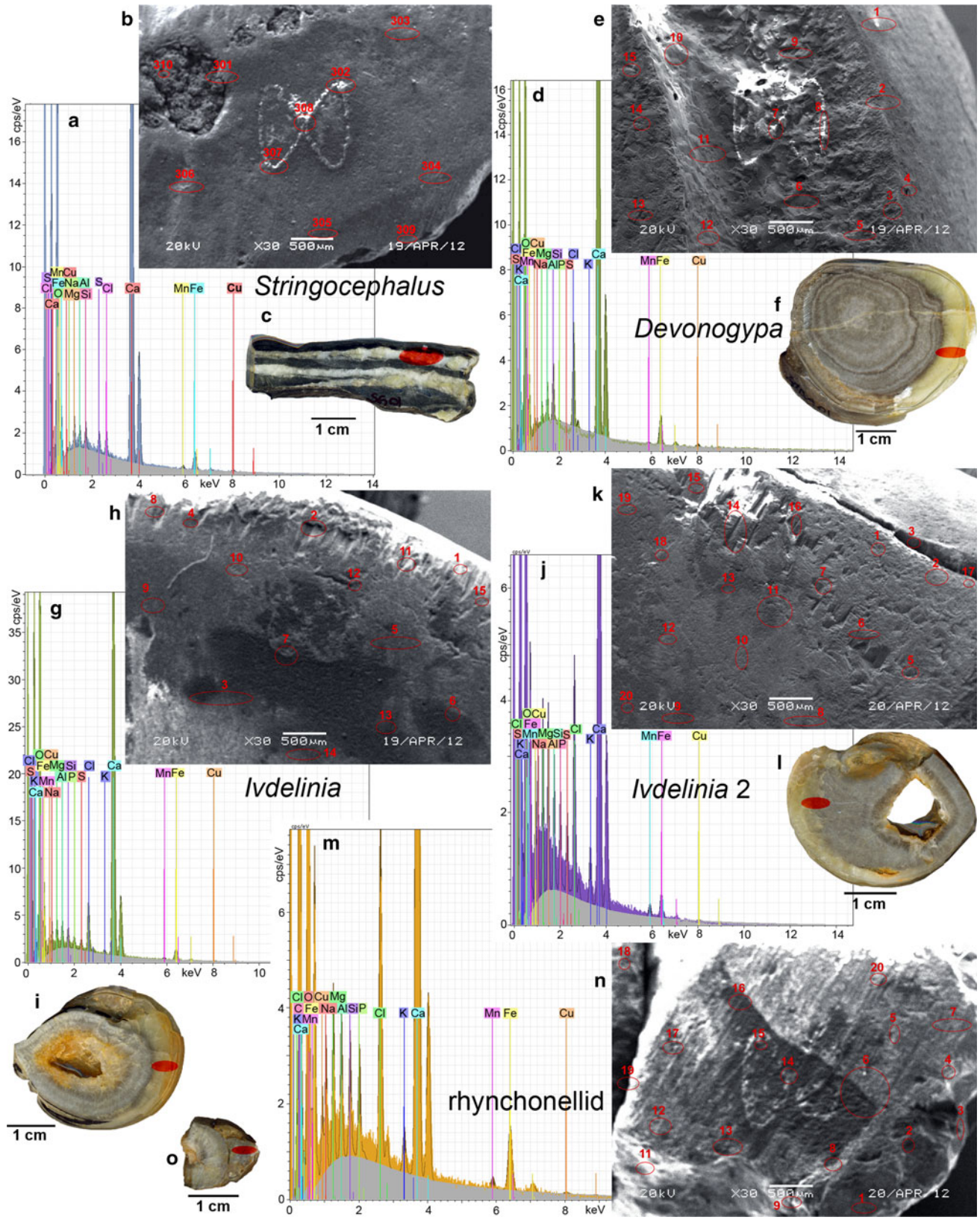

probably, the Cl content results from salt formed by the evaporation of sea-water. Moreover, Mn is present in low to moderate amounts; it was measured with 0.22 wt % only in the innermost part of the shell. The distribution of the Fe and Mn content apparently correlates with the colouring of the sample to some extend.

◀ **Fig. 8** Analyses, SEM images, and photos of the sectioned specimens of the analysed shell parts (measured spot marked by a *red ellipsis*). **a–c** *Stringocephalus* sp., PIMUZ 30218, Givetian, Warstein (Germany); **a** EDX Spectrometer of Object 308; **b** SEM image with the measured surfaces with object numbers; **c** image of sectioned surface. **d–f** *Devonogypa* sp., PIMUZ 30214, Givetian, Aferdou El Mrakib (Morocco); **d** EDX Spectrometer of Object 11; **e** image with the measured surfaces with object numbers; **f** image of sectioned surface. **g–i** *Ivdelinia pulchra,* PIMUZ 30215, Givetian, Aferdou El Mrakib (Morocco); **g** EDX Spectrometer of Object 7; **h** image with the measured surfaces with object numbers; **i** image of sectioned surface. **j–l** *Ivdelinia pulchra* 2, PIMUZ 30216, Givetian, Aferdou El Mrakib (Morocco); **j** Spectrometer of Object 11; **k** image with the measured surfaces with object numbers; **l** image of sectioned surface. **m–o** unidentified rhynchonellid, PIMUZ 30217, Givetian, Aferdou El Mrakib (Morocco); **m** EDX Spectrometer of Object 15; **n** image with the measured surfaces with object numbers; **o** image of sectioned surface

Ivdelinia pulchra

The colour of the shell of *Ivdelinia pulchra* (PIMUZ 30215 and 30216; Fig. 8g–i) varies from greenish to yellowish to greyish. Generally, the shells of this brachiopod exhibit the lowest measured values in Fe (0.28–0.48 wt %) and Mn (0–0.37 wt %). The mean values of Fe (Table 2, online material) exceed those of Mn in all examined brachiopods with the exception of one measurement in *Ivdelinia pulchra* (PIMUZ 30215). This exceptional finding might explain the slightly more yellowish colour of the shell compared to the green shells of *Devonogypa* sp. and *Stringocephalus* sp. *Ivdelinia pulchra* was also analysed from the surface towards the inner part of the shell (Fig. 8g–i). On the surface (Objects 1, 2, 11, 15) of the thin-shelled *Ivdelinia pulchra* (PIMUZ 30215), Fe is present but in low amounts. By contrast, all other typical shell and clay components were found (C, O, Ca, Mg, Si, Cl, Al, P, Na, K). Towards the inside of PIMUZ 30215 (Objects 3, 7), Fe becomes slightly more pronounced (0.88–1.42 wt %), but Mn contents remain low (0.13–0.24 wt %). In general, the values for these analyses are low except for the elements composing the shell and those originating from clay minerals. The greenish to yellowish colour area in this specimen is less pronounced compared to *Devonogypa* sp. and *Stringocephalus* sp., which coincides with generally low concentrations of Fe.

The second *Ivdelinia pulchra* (PIMUZ 30216) sample has a slightly thicker shell (1 mm) compared to the other *Ivdelinia pulchra* specimen (PIMUZ 30215; Fig. 8j–l) and correspondingly shows higher concentrations of Fe and Mn. On the surface (Objects 1, 2, 4, 17), Fe and Mn have moderately high values (Appendix), while the calcite and clay elements are the major constituent of this part of the shell. Inwards (Objects 7, 10, 11, 13, 14, 15; Appendix), the amounts of Fe and Mn increase. Cl is the major component after the calcite-elements (C, O, Ca), which could indicate a high presence of salt in the form of solid incrustations in the shell. Towards the inside of the shell (Objects 8, 9), Fe as well as Mn becomes more important,

Table 1 Measurements of green values (from RGB-images) versus Fe content (wt %)

Stringocephalus	Fe	V	*Devonogypa*	Fe	V	*Ivdelinia (1)*	Fe	V	*Ivdelinia* (2)	Fe	V	Rhynchonellid	Fe	V
Object 301	38.44	27	Object 1	0.17	127	Object 1	0.07	145	Object 1	0.42	84	Object 1	0.97	76
Object 302	2.68	116	Object 2	0.60	141	Object 2	0.18	164	Object 2	0.38	91	Object 2	0.81	84
Object 303	1.58	120	Object 3	1.16	139	Object 3	0.88	82	Object 3	0.38	97	Object 3	0.25	108
Object 304	1.47	129	Object 4	0.42	134	Object 4	0.06	139	Object 4	0.48	104	Object 4	0.49	81
Object 305	1.38	126	Object 5	1.84	115	Object 5	0.18	134	Object 5	0.08	69	Object 5	0.00	78
Object 306	2.12	121	Object 6	2.13	126	Object 6	0.45	110	Object 6	0.04	77	Object 6	0.03	78
Object 307	2.56	136	Object 7	1.30	113	Object 7	1.42	94	Object 7	0.26	76	Object 7	0.22	58
Object 308	2.16	118	Object 8	1.17	158	Object 8	0.09	131	Object 8	1.12	67	Object 8	0.25	73
Object 309	1.70	139	Object 9	0.76	106	Object 9	0.00	78	Object 9	0.98	66	Object 9	0.63	59
Object 310	64.04	70	Object 10	1.79	92	Object 10	0.03	113	Object 10	0.46	56	Object 11	0.29	105
			Object 11	1.74	72	Object 11	0.05	164	Object 11	0.64	67	Object 12	0.10	93
			Object 12	2.10	58	Object 12	0.04	144	Object 12	0.42	65	Object 13	1.01	69
			Object 13	0.40	47	Object 13	0.01	106	Object 13	0.58	74	Object 14	0.27	79
			Object 14	0.48	52	Object 14	0.42	70	Object 14	0.17	77	Object 15	1.38	88
			Object 15	0.44	53	Object 15	0.29	149	Object 15	0.20	87	Object 16	0.58	87
									Object 16	0.47	73	Object 17	1.13	65
									Object 17	0.67	90	Object 18	1.15	100
									Object 18	0.30	63	Object 19	2.74	40
									Object 19	0.58	85	Object 20	0.01	68
									Object 20	0.96	88			

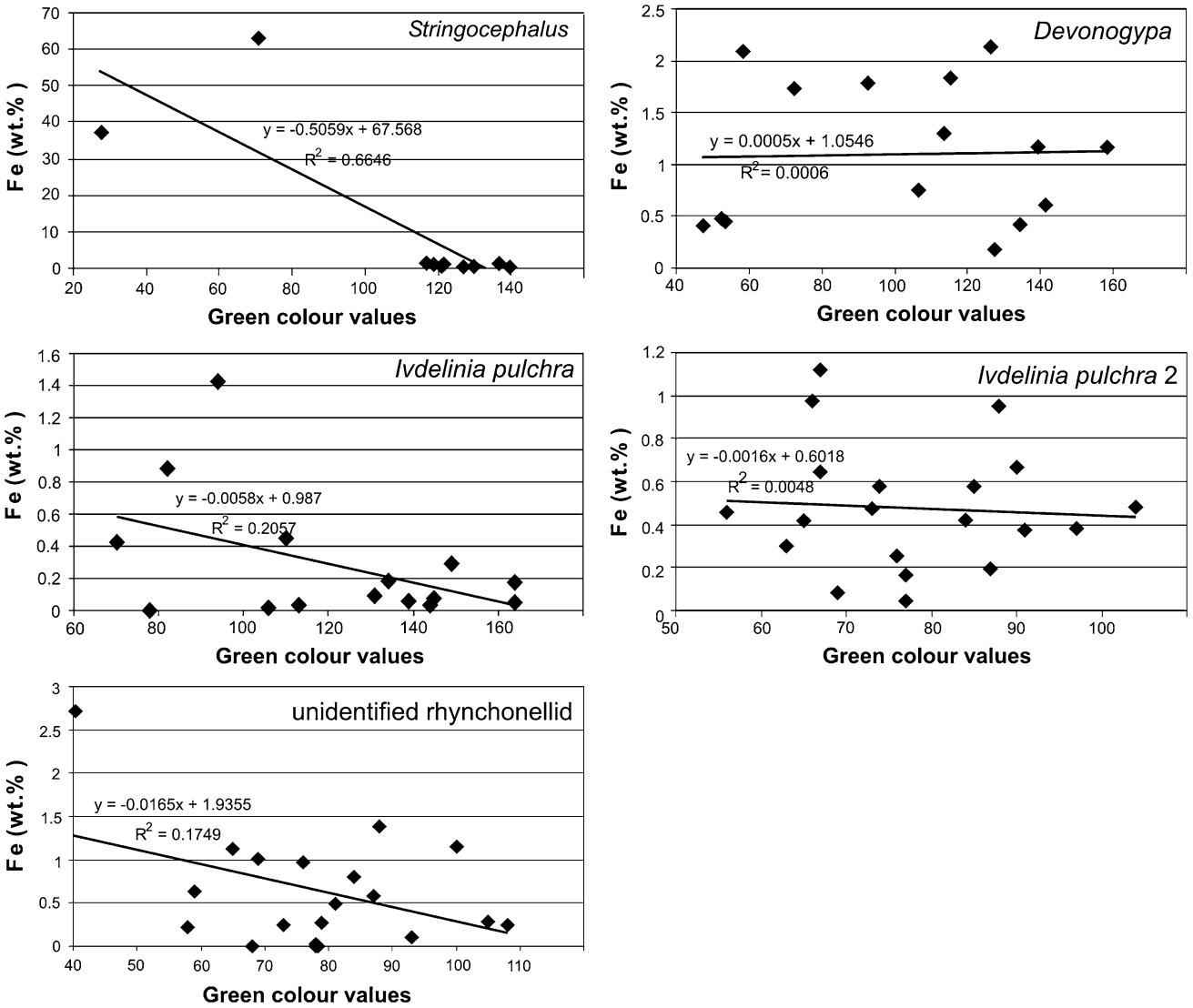

Fig. 9 Correlation between the Fe concentration in the shell and the *green surface-colour* on *Stringocephalus* sp., (Germany), *Devonogypa* sp., (Morocco), two specimens of *Ivdelinia pulchra* (Morocco) and the rhynchonellid (Morocco)

but the values of Mn remain low. The Cu-artefact is again omnipresent in our analyses and increases slightly from the surface inwards. The thicker shell compared to the other *Ivdelinia pulchra* could explain the higher values of the shell components (C, O, Ca, Na, Mg, Si, P, S, Cl, K, Mn, and Fe) and the conspicuous change in Fe concentration. Moreover, the shell is coloured more greenish compared to the other more yellowish specimen of *Ivdelinia pulchra* (PIMUZ 30215).

Undetermined rhynchonellid brachiopod

A 2 cm long undetermined rhynchonellid brachiopod (PIMUZ 30217; Fig. 8m–o) with a thin greyish shell has been analysed. In this specimen, the concentration of Fe is slightly lower (0.64 wt %) compared to *Devonogypa* sp. and much lower when compared to *Stringocephalus* sp., but it still contains Fe.

The main elements composing the surface of the shell (Objects 1, 2, 3 in Fig. 8; Appendix) are Ca, Si, and Al. Towards the inner part of the shell, Cl becomes more abundant while Fe increases to 1–2 wt % (Fe) and Mn to 0.3 wt %. The shell of this brachiopod is thin but shows higher concentrations of Fe, Mn, Cu, Ca, K, P, Si, Al, and C than that of *Ivdelinia pulchra*, but it is greyish (less greenish than *Ivdelinia*).

Element composition and colouration of the shell

As documented by Hassan (1978) for inorganically formed calcite crystals and later by Klug et al. (2009) for trilobite

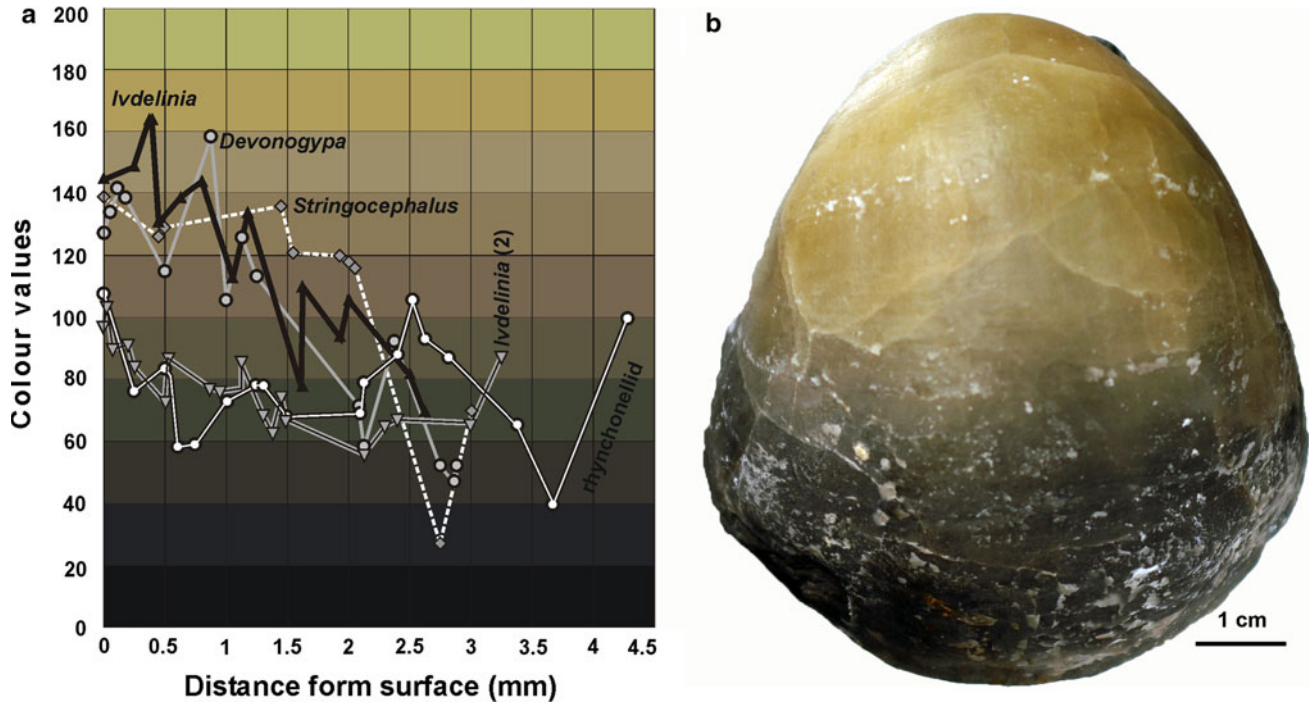

Fig. 10 Shell colour and shell thickness. **a** Correlation of the *green shell colour* (*RGB green values*, measured in PhotoShop) with the distance from the surface in the *Stringocephalus* sp., *Devognogypa* sp., *Ivdelinia pulchra*, and undetermined rhynchonellid brachiopod specimens from Germany and Morocco. **b** *Devonogypa* sp., PIMUZ 30141, Givetian mound facies of the northwestern flank of Aferdou El Mrakib, Maïder, Morocco. Note the change in colour from the umbo, where the shell is the thickest, to the commissure, where the shell has the lowest thickness

eye lenses (see also Lee et al. 2007, 2012 for details of trilobite lens biomineralisation), calcite crystals may become reddish or greenish through impurities of Fe. Even low concentrations of Fe may visibly alter the colour appearance of calcite crystals (see also Kobluk and Mapes 1989). The question arose, whether the Moroccan gypidulids described herein are also green because of such iron impurities and why, in the same strata, some brachiopods show green shells while others are grey like the sediment matrix.

C, O, and Ca are the most abundant components of the shells, which is not surprising, since they are the main primary components of the brachiopod shells (see, e.g., Brand et al. 2003). Mg is common as well because of the preservation of significant parts of the primary composition of the low-Mg-calcitic shell. The presence of P is likely due to remains of organic matter. K, Cl, S, Na, and Al (partially biased from the measurement conditions) are clay and salt components, the latter being not directly relevant for the colour. Locally, the analyses indicate high levels of Cl and Na, which are related solid inclusions of salt (NaCl) in the brachiopod shells. This is supported by the fact that such solid inclusions of salt can be formed at low temperatures on the surface and not under the high temperatures like fluid inclusions. It is also conceivable that they represent younger secondary deposits like calcrete (common in arid environments like the study area in Morocco) deposited by the evaporation of salt-bearing groundwater circulating in cracks in the fossils. This would be not so surprising since many caves are present in the reef mound, representing pathways for groundwater and also rainwater.

Thick shells like those of *Stringocephalus* sp. and *Devonogypa* sp. exhibit about 1–2 wt % of Fe and 0.5–0.15 wt % of Mn, respectively. By contrast, the thinner shells contain between 0.3 and 0.6 wt % of Fe and between 0.1 and 0.2 wt % of Mn. Mn^{2+} and Fe^{2+}-ions originally have a pink and brownish to greenish colour. Among the found elements, Fe^{2+} is the only element that may cause the characteristic greenish colour of these brachiopods in the low measured concentrations (cf. Hassan 1978). Fe^{2+} is common in oceanic as well as in continental crust, in several mollusk shells (*Anodonta, Nucula sulcata,* etc.; Swinehart and Smith 1979), but also in the phreatic zone and in hydrothermal sources. A reducing environment (RED) indicating a temporary diminution of sea water oxygenation could also explain the presence of Fe^{2+} in the brachiopod shells; nevertheless, other indicators for low-oxygen-conditions are missing in the reef mound sediments. A hypothesis to generate anoxic conditions is the decomposition of dead organisms, which may cause a drop in oxygen. For instance, it may lead to the conservation of

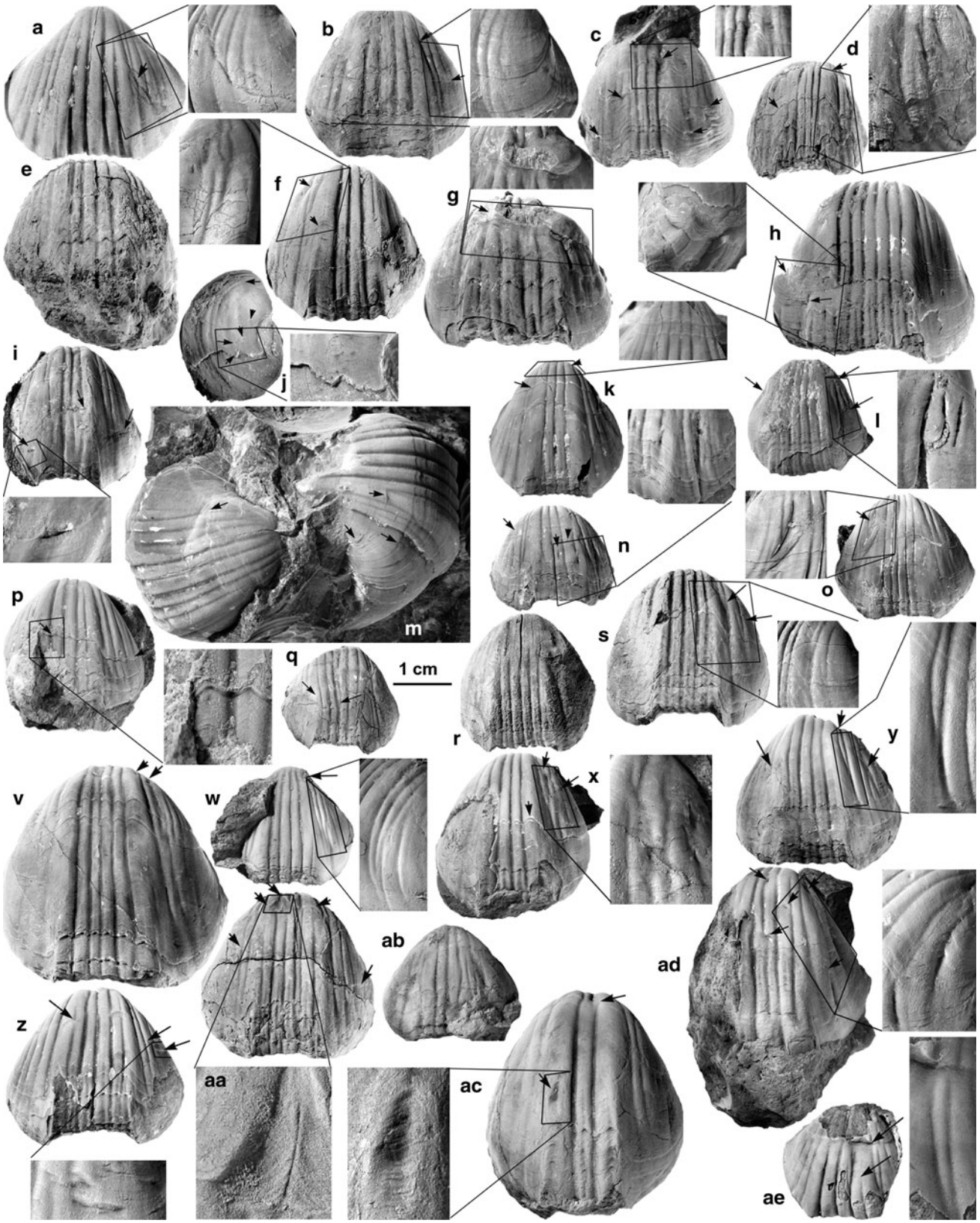
a
b
c
d
e
f
g
h
i
j
k
l
m
n
o
p
q
1 cm
r
s
x
y
v
w
ab
ad
z
aa
ac
ae

◀ **Fig. 11** Some specimens of *Ivdelinia pulchra* with healed sublethal injuries. Givetian mound facies of the northwestern flank of Aferdou El Mrakib, Maïder, Morocco. *Arrows* mark the injuries. All specimens × 1, coated with NH_4Cl. Note that (1) many injuries occur on the flanks, (2) many injuries are small, (3) injuries on both sides are common, (4) intraspecific variability is very high, partially due to the deformities. **a** PIMUZ 30023, **b** PIMUZ 30025, **c** PIMUZ 30028, **d** PIMUZ 30034, **e** PIMUZ 30036, **f** PIMUZ 30039, **g** PIMUZ 30040, **h** PIMUZ 30042, **i** PIMUZ 30045, **j** 30049, **k** PIMUZ 30060, **l** PIMUZ 30063, **m** PIMUZ 30051–30052, **n** PIMUZ 30164, **o** PIMUZ 30173, **p** PIMUZ 30170, **q** PIMUZ 30176, **r** PIMUZ 30187, **s** PIMUZ 30180, **v** PIMUZ 30190, **w** PIMUZ 30099, **x** PIMUZ 30101, **y** PIMUZ 30104, **z** PIMUZ 30107, **aa** PIMUZ 30108, **ab** PIMUZ 30127, **ac** PIMUZ 30122, **ad** PIMUZ 30123, **ae** PIMUZ 30128

mammoth teeth in vivianite (Fe^{2+}) or other phosphates (Fe^{3+}), which give a blue colour. In a RED system, the organic matter is relatively abundant, and the Fe^{2+}-ions could be linked to other free ions in the environment, in order to form a stable molecule, like, for instance, pyrite. A ferrous phosphate such as $Fe_3(PO_4)_2$ (or other molecules) could be another source for Fe^{2+} ions, even if in general, the iron-phosphate is slightly soluble, and it is easier to find vivianite ($Fe_3(PO_4)_2 \cdots 8H_2O$; blue colour).

Growth of the carbonate build-ups in the eastern Anti-Atlas has repeatedly been suggested to be caused by hydrothermal activity (Belka 1994, 1998; Aitken et al. 2002; Berkowski 2006; Cavalazzi et al. 2007). As far as the Aferdou El Mrakib reef mound is concerned, hydrothermalism as cause for the mound formation has also been discussed by Kaufmann (1998). Kaufmann noted (1998: p. 95) that "NE-SW-trending dolomitized joints, which are attributed to the Variscan fault system" cross the Aferdou El Mrakib mound as well as its neighbour, Guelb El Maharch. These might have represented sources of hydrothermal fluids delivering Fe^{2+} ions. In the presence of large amounts of carbonate, Fe^{2+} ions can form yellow siderite ($FeCO_3$) but also clay minerals such as the green ferrosaponite ($Ca_{0.3}(Fe^{2+}, Mg, Fe^{3+})_3[(OH)_2|(Si, Al)Si_3O_{10}] \cdots 4H_2O$) and these may be precipitated in shells. Some clay minerals such as ferrosaponite are known from calcite crystals and that they form in hydrothermal contexts. There is probably a low lower limit of iron content needed to obtain a greenish colour (Fig. 9); a percentage of 1–2 wt % can visibly change the colour of the shell.

In accordance with the findings of Hassan (1978), the pale greenish colour of the thick-shelled brachiopods both from Morocco and from Germany can be attributed to the presence of Fe^{2+} ions. These ions mask the pale pink colour expected to occur due to the presence of Mn^{2+} ions substituting Ca^{2+} ions in the calcite structure. Moreover, it is known that CO_2 dissolved in sea water can lead to the decomposition of the bicarbonate and to the formation of $CaCO_3$, which is deposited as calcite at a pH of 7.8 or more (Hassan 1978). That means that the presence of Fe^{2+} and Mn^{2+} ions demands an acidic or reducing environment. Otherwise, the Fe^{2+} ions would have been readily oxidised to Fe^{3+} (Hassan 1978). The Fe^{2+} is here considered as being bound in a mineral and not directly related to the calcite composition of the shell.

What controls the intensity of the colour? We assessed this question by comparing the amount of Fe with the intensity of the colour and with the distance of the measured Fe from the shell surface (Figs. 9, 10). It turned out that even a very low Fe concentration could change the colour in the shells, as mentioned earlier (Fig. 9), because there is only a moderate correlation between the colour and the Fe content ($r = 0.574215$, $p = 0.0650251$). Nevertheless, there appears to be a correlation between the variation of the green colour and the shell thickness, as reflected by the moderate correlations of the distance of the measured surface from the shell surface with the Fe content (Fig. 10) and by the fact that large *Devonogypa* specimens have a more greyish shell near the commissure opposite of the umbo (where the shell is thin) than on the umbo itself, where the shell may reach a thickness of around 1 cm. We thus conclude that the green colour depends less on the Fe^{2+} concentration (0.2 wt % is probably already sufficient) than on the shell thickness. Indeed, large specimens of both *Ivdelinia pulchra* and *Devonogypa* sp. are greener than smaller specimens (Fig. 8), which is also supported by the grey colour of the examined rhynchonellid and of the thin shells of co-occurring atrypids.

Sublethal injuries and the palaeoecology of the gypidulids

Sublethal injuries and shell deformations are common in Palaeozoic brachiopods and also in other invertebrates (Signor and Brett 1984; Bambach 1999; Nützel and Frýda 2003; Klug 2007; Klug et al. 2010; Slotta et al. 2011). The Devonian is commonly characterised by the explosive radiation of nektonic organisms such as jawed fish and ammonoids. A rapid occupation of the free water column by swimming organisms (mostly predators) occurred at that time (Klug et al. 2010).

Here, we document healed injuries in the shells of the two brachiopod genera *Ivdelinia* and *Devonogypa* (Figs. 3, 4, 6, 10, 11, 12) to obtain some information on their palaeoecology. As mentioned in "Methods", many different kinds of sublethal injuries have been found. Although it is almost impossible to assign certain types of injuries to distinct predators or other causes, the diversity in healed injuries still sheds some light on the habitat of these brachiopods. As far as possible causes for the injuries are concerned, these might have been failed attacks of (1) vertebrate or (2) invertebrate predators or shell damage

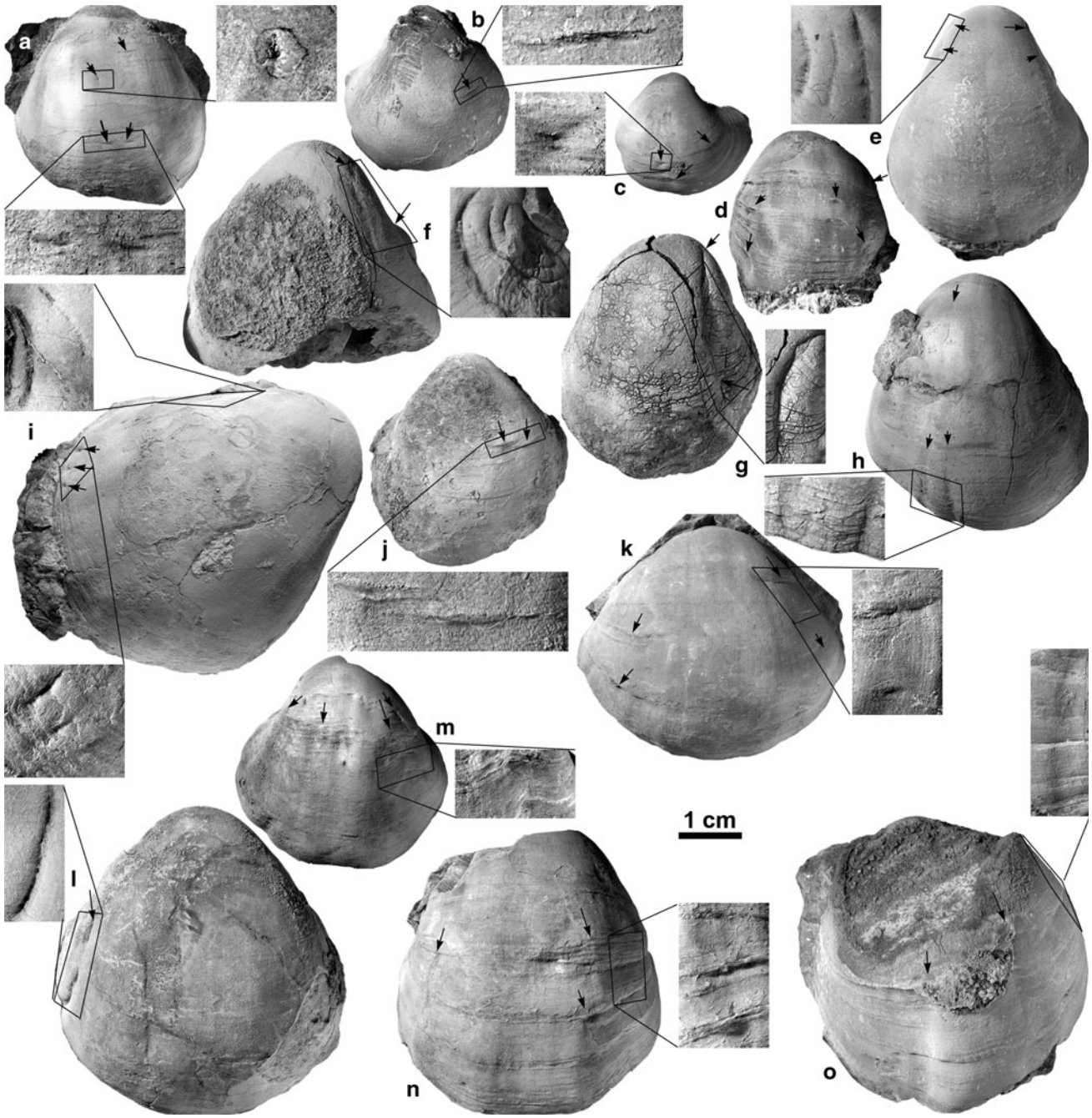

Fig. 12 Some specimens of *Devonogypa* sp. with healed sublethal injuries. Givetian mound facies of the northwestern flank of Aferdou El Mrakib, Maïder, Morocco. *Arrows* mark the injuries. All specimens × 1, coated with NH_4Cl. Note that (1) many injuries occur on the flanks, (2) many injuries are small, (3) injuries on both sides are common, (4) intraspecific variability is very high, partially due to the deformities. **a** PIMUZ 30131, **b** PIMUZ 30137, **c** PIMUZ 30138, **d** PIMUZ 30139, **e** PIMUZ 30161, **f** PIMUZ 30148, **g** PIMUZ 30150, **h** PIMUZ 30152, **i** PIMUZ 30162, **j** PIMUZ 30076, **k** PIMUZ 30208, **l** PIMUZ 30066, **m** PIMUZ 30213, **n** PIMUZ 30198, **o** PIMUZ 30091

might have occurred by (3) shells hitting each other in an environment with moderately strong to strong water movements (e.g., above the wave base) or (4) during gravitational displacement of specimens.

1. Fossils of vertebrate predators are exceedingly rare on Aferdou El Mrakib. Kaufmann (1998) mentioned rare finds of isolated minute phoebodontid shark teeth. In addition, brachiopods are not an attractive prey for sharks and most other predators, partially because of the poor soft-tissue/shell-ratio (and in the case of the studied brachiopods, the shell is very thick). Vertebrates cannot be ruled out as causers of some injuries

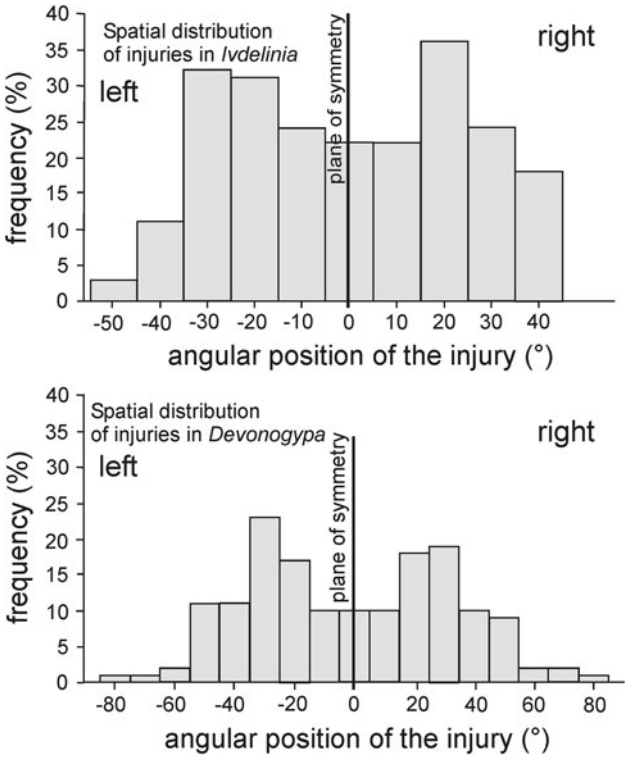

Fig. 13 Frequency of injuries in the two gypidulid brachiopods from the Aferdou El Mrakib (Morocco). Their angular position is measured relative to the plane of symmetry on ventral valves only. *Top Ivdelinia pulchra* (number of specimens: 110; number of injuries: 180), Morocco. *Bottom Devonogypa* sp. (number of specimens: 82; number of injuries: 144)

but they probably were responsible for injuries only in very rare cases.

2. As far as invertebrate predators are concerned, cephalopods are worth mentioning. Ammonoid remains are exceedingly rare in the mound sediments while the loosely coiled shells (up to 15 cm shell diameter) of rutoceratids are moderately common. Cephalopods are known to be capable of producing paired fractures with their beaks (Sarycheva 1949; Saunders et al. 1978; Alexander 1986; Elliott and Bounds 1987; Elliott and Brew 1988; Klug 2007 and references therein). Therefore, the paired injuries can be assigned to cephalopod predators with some reservation.
3. Gravitational displacement of brachiopod shells certainly occurred on Aferdou El Mrakib, which is documented in massive debris deposits on the flanks and around the reef mound. In many cases, such displacements will have caused burial and thus death of the affected individuals.
4. Our favoured hypothesis for the majority of the often small injuries is thus that these two brachiopod species occurred in dense populations, where the shells hit (or rubbed against) each other even during moderate water movements, causing small shell fractures near the commissure. We thus investigated the distribution of the damages over the shell relative to the plane of symmetry.

Distribution of the injuries

In *Devonogypa* sp. and *Ivdelinia pulchra*, the injuries occur mostly in the ventral valves. The dorsal valves are apparently affected by these fractures less commonly, which can be explained by its flat shape and its much smaller surface. Therefore, only the fractures on the ventral valves were evaluated and counted.

As visible in the plate in Fig. 11, the frequency of injuries in *Ivdelinia* is low in the central part, as well as on the parts farthest from the plane of symmetry (see also Fig. 13). Conversely, in the lateral parts, between 15 and 35° from the plane of symmetry, the frequency of injury is higher.

Concerning the appearance of the injuries in *Ivdelinia*, it is noticeable that some injury types appear only in pairs (types 3–5) and often symmetrically (Figs. 6, 11). Furthermore, the shells often possess more than two injuries of different types.

In *Devonogypa* (Figs. 4, 12, 13), the distribution of injuries is similar. The abundance of injuries near the plane of symmetry is slightly lower than on the flanks. In *Devonogypa* specimens, different types of injuries also occur (Fig. 12). They often lie in the zones between 15° and 35° from the plane of symmetry.

The distribution, which shows a differentiation between the central part and the flank between 15 and 35°, is probably due to the fact that the lower part of the shells (aperture) is more protected than in the *Ivdelinia pulchra* shells.

It is noteworthy that several representatives of both taxa show repeated malformations on both sides in several specimens (Figs. 11c, d, f, j, aa, 12d, f, m–o). These point at a more or less continuous irritation of the mantle, which might have occurred in dense populations, where the shells rubbed against each other in gentle water movement (e.g., Fig. 12d, n) or, in the case of strong currents (storms, submarine slides etc.), they would have hit each other, thus breaking the shell and causing more serious injuries (e.g., Figs. 11h, 12e). This is even more likely when one considers possible modes of life of these gypidulids. As gypidulids, these brachiopods belong to the Pentameridina, and according to Boucot (1975), these lived typically within the photic zone. The pedicle was reduced since the pedicle foramen

is closed. One possibility is that these brachiopods lay with the ventral valve (especially the umbonal side) facing downward on the sediment. The weight of the thick umbonal part of the ventral valve gave some stability to this position, somewhat comparable to the Jurassic bivalve *Gryphaea* (e.g., Hallam 1968). Presuming this is true, the downward orientation of the ventral valve would explain, why the central part was less affected by injuries to some extent.

Table 2 Measurements of the angular distance of injuries from the plane of symmetry of *Devonogypa* and *Ivdelinia*, respectively

Ivdelinia			
n (specimens)	94		
n (without injuries)	16		
n (with injuries)	78		
Injuries/*n* (specimens)	2,553,191		
Injuries/*n* (with injuries)	3,076,923		
Angle	Left	Right	
0–5	0	0	
5–15	0	0	
15–25	0	0	
25–35	0	0	
35–45	3	0	
45–55	11	18	
55–65	32	29	
65–75	31	36	
75–85	24	22	
85–90	21	13	
Sum	122	118	240
Devonogypa			
n (specimens)	78		
n (without injuries)	23		
n (with injuries)	55		
Injuries/*n* (specimens)	2,025,641		
Injuries/*n* (with injuries)	2,872,727		
Angle	Left	Right	
0–5	0	0	
5–15	1	1	
15–25	1	2	
25–35	2	2	
35–45	11	9	
45–55	11	10	
55–65	23	19	
65–75	17	18	
75–85	10	10	
85–90	5	6	
Sum	81	77	158

Remarkably, most of the specimens of the two brachiopod genera in our sample show small sublethal injuries. 158 injuries have been detected in 78 *Devonogypa* sp. specimens and 240 injuries in 94 *Ivdelinia pulchra* specimens. In 23 specimens of *Devonogypa* and in 16 specimens of *Ivdelinia*, no injuries were seen, either because the surface was corroded or because none were present. On average, each specimen carries more than two injuries (Table 2). This shows that the individuals of both genera were exposed to hazards (water movement, predation) to similar degrees and therefore support the hypothesis that they occupied similar habitats. In *Ivdelinia* and *Devonogypa*, the same types of injuries occur, additionally corroborating similarities in their palaeoecology. Common causes can, therefore, be assumed for both taxa, which may have varied from predators (Signor and Brett 1984), to transport and contact with other shells, sediment particles, etc.

The fact that injuries are more abundant on the flanks than in the central 30° wide sector (almost twice as much per 10° in *Devonogypa* and still about 30 % more in *Ivdelinia*) supports the hypothesis that the sides of the shells hit each other in dense populations. Although not quantified, a strong variability in the shell length to width ratio is visible. This might also be a result of these dense populations. Ultimately, the great abundance of these brachiopods on the reef mound and its scarcity in the off-mound facies further corroborate this interpretation.

Conclusions

Ivdelinia pulchra and *Devonogypa* sp. are the most abundant and thus the most characteristic brachiopods on and in the Moroccan Aferdou El Mrakib reef mound. *Stringocephalus* sp. is similarly abundant in the shallow water limestone facies of Germany. These three genera have in common, that locally, their shells display a greenish colour. Our chemical analyses yielded differences in the mean values of the weight percentages of certain elements in the shells of these brachiopods. The concentrations of certain elements such as Fe and Mn increase from the surface to the inside of the shells. It is the Fe^{2+}-ions, which are responsible for the green colour. This element is associated with a reducing system (RED), probably related with a hydrothermal source, where Fe^{2+} had the possibility to bind with other ions, possibly within clay minerals, for example, of the illite or montmorillonite groups. Several solid salt inclusions have also been found, especially in the

shell of *Devonogypa*, in the undetermined thin-shelled rhynchonellid, and in one of the *Ivdelinia pulchra* specimens. In addition, it showed that the colour is largely independent of the Fe^{2+}-concentration itself (as long as it is present) and is mainly determined by shell thickness, thus the limitation of the green colour to thick-shelled brachiopods. In future studies, the minerals responsible for the green colour could be determined.

Our analysis of non-lethal injuries showed that over two-thirds of the shells of both *Devonogypa* sp. and *Ivdelinia pulchra* have been damaged syn vivo. Although a few of the injuries might have been inflicted by rare vertebrate predators and some (paired holes) might have been caused by invertebrates (non-ammonoid cephalopods), we suggest that the majority was formed by rough contacts between brachiopod shells in dense populations of these two genera. Their mass occurrences were probably due to a hospitable environment characterised by more or less shallow water (photic zone), moderate water energy (which ensured the steady availability of enough nutrient and oxygen), normal salinity, and a habitat more or less protected from maximum water energy. The great abundance of injuries contributes also to the great intraspecific variability of both gypidulid taxa, since injuries inflicted early in ontogeny might have caused profound changes in adult shell morphology. In any case, we suggest that this variability is also a consequence of the great density of the populations. Intraspecific variability of these brachiopods still needs to be quantified. Whether these gypidulids behaved similar to or differently from other brachiopods in these respects could be the subject of future studies.

Acknowledgments We greatly appreciate the support by the Swiss National Science Foundation (Project numbers 200021-113956/1, 200020-25029, and 200020-132870). Kenneth De Baets (Bristol) and Richard Hofmann (Zürich) contributed some of the specimens. Our colleagues Markus Hebeisen, Rosmarie Roth, Christian Kolb and Beat Scheffold (Zurich) supported us with various work in the lab. Axel Munnecke (Erlangen) contributed for the brachiopod environment deposition interpretation. Torsten Vennemann (Lausanne) supported and contributed to the geochemical analyses interpretation. Michael Hautmann (Zürich) read the manuscript and provided some important hints, which helped much to improve the manuscript. James Neenan (Zürich) kindly revised the English in the manuscript. The constructive comments of the two reviewers Art Boucot (Corvallis) and Robert B. Blodgett (Anchorage) are greatly appreciated.

Appendix

See Table 3.

Table 3 EDX-analyses of the brachiopod shells in wt %

Stringocephalus	C	O	Na	Mg	Al	Si	P	S	Cl	K	Ca	Mn	Fe	Cu
Object 301	23.522	47.757	0.042	0.074	0.073	0.010	0.000	0.181	0.386	0.036	9.834	0.561	38.435	1.101
Object 302	35.594	96.404	1.135	1.511	0.872	0.606	0.500	0.541	1.420	0.279	31.521	0.553	2.678	0.431
Object 303	75.530	168.989	3.064	3.538	2.899	2.202	2.038	1.675	4.597	1.179	24.389	0.698	1.581	0.002
Object 304	49.812	100.728	1.147	1.442	1.179	0.730	0.643	0.604	0.776	0.482	30.060	0.589	1.469	0.221
Object 305	25.156	65.226	0.132	0.326	0.148	0.090	0.122	0.125	0.143	0.100	38.459	0.339	1.381	0.865
Object 306	50.912	111.160	1.430	1.855	1.338	0.982	0.804	0.744	1.945	0.000	30.794	0.481	2.120	0.325
Object 307	31.335	82.996	0.823	1.053	0.599	0.438	0.366	0.439	0.755	0.228	34.507	0.448	2.561	0.556
Object 308	23.131	60.146	0.240	0.581	0.367	0.374	0.000	0.414	0.589	0.000	33.763	0.401	2.159	0.374
Object 309	28.714	52.423	0.247	0.250	1.605	0.159	0.021	0.073	0.213	0.174	31.867	0.000	1.700	1.208
Object 310	9.659	26.256	0.000	0.001	0.010	0.031	0.000	1.931	0.172	0.008	0.715	0.000	64.038	1.106
Mean value	30.376	68.058	0.860	1.042	0.919	0.593	0.396	0.694	1.052	0.248	29.149	0.509	11.329	0.586
Sigma	17.127	34.236	0.913	1.009	0.868	0.674	0.505	0.707	1.300	0.282	21.651	0.115	20.141	0.394
Sigma mean	3.830	7.655	0.204	0.226	0.194	0.151	0.113	0.158	0.291	0.063	4.841	0.026	4.504	0.088
Devonogypa	C	O	Na	Mg	Al	Si	P	S	Cl	K	Ca	Mn	Fe	Cu
Object 1	22.362	54.419	0.604	0.318	0.181	0.126	0.016	–	0.085	0.060	20.948	0.115	0.171	0.595
Object 2	23.101	50.146	0.352	0.346	1.004	1.576	0.011	–	0.158	0.174	21.191	0.135	0.601	1.203
Object 3	23.327	47.256	0.194	0.309	1.044	1.827	0.017	–	0.150	0.199	22.849	0.214	1.165	1.449
Object 4	24.731	48.858	0.187	0.113	0.808	0.252	0.000	0.001	0.086	0.058	23.488	0.114	0.419	0.883
Object 5	19.688	49.012	0.049	0.289	1.632	2.730	0.001	0.000	1.031	0.269	22.306	0.206	1.838	0.949
Object 6	23.075	40.490	0.000	0.000	0.167	0.146	0.000	0.000	1.190	0.009	31.603	0.157	2.132	1.031
Object 7	18.555	50.050	0.127	0.230	0.709	1.270	0.009	0.003	0.933	0.045	25.929	0.169	1.301	0.672

Table 3 continued

Devonogypa	C	O	Na	Mg	Al	Si	P	S	Cl	K	Ca	Mn	Fe	Cu
Object 8	18.825	48.410	0.005	0.071	0.697	1.228	0.000	0.000	0.517	0.041	27.143	0.104	1.169	1.791
Object 9	21.775	49.972	0.099	0.201	0.836	1.424	0.002	0.001	0.299	0.070	23.767	0.124	0.758	0.671
Object 10	18.668	53.181	0.336	0.221	0.178	0.088	0.015	0.001	1.210	0.009	23.816	0.062	1.794	0.422
Object 11	19.684	53.076	0.288	0.308	0.462	0.624	0.015	0.002	1.221	0.018	22.091	0.081	1.741	0.390
Object 12	19.371	51.138	0.236	0.190	0.304	0.544	0.000	0.004	1.146	0.012	24.335	0.089	2.100	0.532
Object 13	22.120	51.204	0.496	0.373	0.276	0.204	0.105	0.087	0.154	0.131	23.753	0.224	0.398	0.475
Object 14	18.253	49.146	0.178	0.139	0.069	0.083	0.005	0.009	0.082	0.054	30.487	0.214	0.477	0.806
Object 15	19.974	50.388	0.324	0.297	0.190	0.158	0.077	0.044	0.132	0.070	27.055	0.221	0.444	0.625
Mean value	20.901	49.783	0.232	0.227	0.570	0.819	0.018	0.013	0.560	0.081	24.717	0.149	1.101	0.833
Sigma	2.112	3.216	0.173	0.108	0.442	0.812	0.031	0.026	0.492	0.078	3.170	0.056	0.684	0.399
Sigma mean	0.545	0.830	0.045	0.028	0.114	0.210	0.008	0.007	0.127	0.020	0.818	0.014	0.177	0.103
Ivdelinia	C	O	Na	Mg	Al	Si	P	S	Cl	K	Ca	Mn	Fe	Cu
Object 1	40.169	51.075	0.985	0.618	0.585	0.379	0.285	–	0.334	0.155	5.242	0.080	0.072	0.021
Object 2	33.935	54.999	0.982	0.723	0.775	0.476	0.418	–	0.584	0.292	6.518	0.093	0.177	0.031
Object 3	25.368	55.359	0.806	0.708	0.641	0.449	0.361	–	0.918	0.138	14.139	0.134	0.883	0.097
Object 4	35.796	54.956	1.035	0.865	0.882	0.537	0.495	–	0.721	0.269	4.327	0.059	0.058	0.000
Object 5		76.109	3.117	2.645	2.439	1.883	1.763	–	3.016	0.916	7.815	0.101	0.184	0.012
Object 6	30.827	54.024	0.861	0.802	0.697	0.570	0.506	–	0.965	0.269	9.889	0.122	0.452	0.016
Object 7	22.433	53.217	0.886	0.619	0.558	0.432	0.280	0.245	1.256	0.148	18.137	0.236	1.423	0.131
Object 8	35.387	53.213	0.759	0.664	1.037	0.434	0.382	–	0.507	0.238	7.204	0.078	0.095	0.001
Object 9	32.180	58.777	1.268	1.018	0.939	0.648	0.617	–	1.024	0.265	3.260	0.000	0.003	0.000
Object 10	29.982	58.643	1.412	1.197	1.093	0.787	0.827	–	1.444	0.448	4.089	0.045	0.031	0.001
Object 11	32.933	56.354	0.976	0.709	1.466	0.409	0.369	–	0.358	0.185	6.130	0.055	0.049	0.005
Object 12	33.042	56.848	1.117	0.872	0.837	0.592	0.564	–	0.909	0.310	4.863	0.007	0.037	0.001
Object 13	40.732	52.087	0.890	0.730	0.904	0.478	0.396	–	0.586	0.218	2.955	0.010	0.014	0.003
Object 14	88.862	158.705	3.229	2.395	2.097	1.475	1.293	–	1.974	0.584	17.100	0.084	0.422	0.010
Object 15	31.028	56.430	1.080	0.953	0.886	0.665	0.664	–	1.144	0.330	6.374	0.150	0.290	0.005
Mean value	36.620	63.386	1.293	1.035	1.056	0.681	0.615	0.245	1.049	0.318	7.870	0.084	0.279	0.022
Sigma	15.814	27.007	0.782	0.625	0.545	0.427	0.409	0.000	0.697	0.203	4.853	0.062	0.395	0.039
Sigma mean	4.083	6.973	0.202	0.161	0.141	0.110	0.106	0.000	0.180	0.052	1.253	0.016	0.102	0.010
Ivdelinia 2	C	O	Na	Mg	Al	Si	P	S	Cl	K	Ca	Mn	Fe	Cu
1	25.979	56.716	0.838	0.822	0.713	0.535	0.399	0.319	0.987	0.286	11.677	0.250	0.418	0.061
2	29.303	56.062	1.263	0.810	0.737	0.531	0.360	0.282	0.798	0.286	8.978	0.198	0.375	0.017
3	27.511	57.408	1.276	0.580	0.411	0.276	0.095	0.067	0.387	0.134	10.958	0.073	0.384	0.441
4	30.428	54.120	0.807	0.766	0.726	0.503	0.352	0.307	0.818	0.263	10.168	0.189	0.479	0.076
5	29.489	58.446	1.093	0.876	0.858	0.566	0.448	0.346	0.741	0.320	6.667	0.061	0.082	0.007
6	30.500	58.168	1.299	1.076	0.984	0.724	0.568	0.432	1.021	0.421	4.703	0.054	0.042	0.008
7	29.131	57.558	1.136	0.997	0.899	0.665	0.502	0.412	1.161	0.403	6.694	0.185	0.256	0.002
8	20.755	51.930	0.683	0.599	0.443	0.374	0.257	0.136	0.915	0.187	21.832	0.368	1.118	0.406
9	19.292	51.325	0.614	0.596	0.342	0.234	0.184	0.102	0.649	0.144	24.911	0.256	0.978	0.373
10	26.431	57.079	1.215	0.974	0.917	0.661	0.528	0.390	1.173	0.414	9.502	0.248	0.455	0.013
11	26.672	55.883	1.180	0.945	0.833	0.595	0.492	0.388	1.228	0.395	10.443	0.261	0.642	0.043
12	27.756	56.444	1.516	0.976	0.948	0.691	0.501	0.405	0.990	0.475	8.661	0.207	0.420	0.010
13	26.197	55.528	1.459	0.965	0.906	0.739	0.567	0.404	1.274	0.453	10.655	0.258	0.576	0.019
14	29.298	58.195	1.212	0.896	0.782	0.525	0.426	0.309	0.786	0.312	6.975	0.110	0.167	0.008
15	27.780	57.294	1.191	1.029	0.947	0.749	0.565	0.476	1.179	0.495	7.921	0.173	0.197	0.006
16	26.630	55.054	1.036	0.887	0.890	0.671	0.534	0.435	1.352	0.472	11.292	0.259	0.471	0.016

Table 3 continued

Ivdelinia 2	C	O	Na	Mg	Al	Si	P	S	Cl	K	Ca	Mn	Fe	Cu
17	26.067	55.365	0.809	0.574	0.530	0.376	0.213	0.143	0.444	0.140	14.188	0.188	0.666	0.297
18	28.253	57.150	1.428	1.000	0.949	0.728	0.562	0.410	1.075	0.472	7.478	0.196	0.299	0.000
19	26.193	56.170	1.211	0.985	0.921	0.675	0.532	0.389	1.168	0.405	10.509	0.246	0.577	0.020
20	20.110	53.412	0.774	0.893	0.590	0.444	0.323	0.231	1.075	0.231	20.448	0.265	0.955	0.251
Mean value	26.689	55.965	1.102	0.862	0.766	0.563	0.420	0.319	0.961	0.335	11.233	0.202	0.478	0.104
Sigma	3.212	1.986	0.264	0.160	0.200	0.156	0.143	0.122	0.267	0.122	5.321	0.079	0.290	0.153
Sigma mean	0.718	0.444	0.059	0.036	0.045	0.035	0.032	0.027	0.060	0.027	1.190	0.018	0.065	0.034

Rhynchonellid	C	O	Na	Mg	Al	Si	P	S	Cl	K	Ca	Mn	Fe	Cu
1	23.548	47.994	0.314	0.708	2.303	3.906	0.286	–	0.361	0.685	18.173	0.375	0.969	0.379
2	28.593	49.464	0.564	1.120	2.988	4.864	0.417	–	0.396	0.748	9.544	0.277	0.807	0.219
3	35.339	29.081	0.269	0.571	25.660	0.520	0.043	–	0.312	0.059	7.256	0.287	0.246	0.358
4	24.437	49.437	0.602	0.444	0.411	0.588	0.048	–	0.295	0.161	22.113	0.228	0.489	0.748
5	40.838	52.891	1.106	0.787	1.065	0.563	0.407	–	0.398	0.179	1.764	0.000	0.002	0.000
6	34.033	56.543	0.947	0.877	1.062	0.596	0.517	–	0.591	0.258	4.534	0.016	0.027	0.000
7	27.985	53.428	0.612	0.738	0.752	0.670	0.322	–	0.364	0.223	14.489	0.147	0.221	0.050
8	28.905	52.999	0.617	0.782	0.684	0.555	0.362	–	0.352	0.201	14.034	0.170	0.251	0.087
9	31.047	37.371	0.000	0.129	8.722	0.340	0.000	–	0.000	0.058	16.531	0.038	0.633	5.130
11	31.450	40.606	0.107	0.324	9.651	0.435	0.000	–	0.031	0.027	13.197	0.050	0.285	3.837
12	38.849	49.481	0.897	0.863	0.948	0.699	0.539	–	0.667	0.364	6.489	0.095	0.098	0.010
13	32.529	48.039	0.819	0.690	0.615	0.559	0.407	–	0.641	0.253	14.051	0.234	1.008	0.154
14	25.428	52.220	0.556	0.787	0.464	0.320	0.263	–	0.214	0.079	18.965	0.170	0.270	0.264
15	30.351	51.410	1.035	0.918	0.720	0.547	0.514	–	1.745	0.285	10.806	0.214	1.378	0.077
16	33.033	53.258	1.158	1.009	0.803	0.556	0.475	–	1.311	0.250	7.432	0.125	0.577	0.013
17	36.444	48.502	0.870	1.114	0.792	0.633	0.576	–	1.534	0.369	7.711	0.211	1.127	0.119
18	29.634	52.815	0.643	0.807	0.495	0.438	0.225	–	0.394	0.111	12.855	0.161	1.148	0.274
19	27.094	46.423	0.289	0.296	0.641	0.383	0.091	–	0.492	0.213	19.993	0.313	2.738	1.033
20	34.970	56.698	1.002	0.927	1.080	0.657	0.564	–	0.666	0.244	3.185	0.003	0.006	0.000
Mean value	31.290	48.877	0.653	0.731	3.150	0.938	0.319	–	0.566	0.251	11.743	0.164	0.646	0.671
Sigma	4.734	6.780	0.341	0.272	6.064	1.230	0.200	–	0.471	0.191	5.900	0.110	0.665	1.387
Sigma mean	1.086	1.555	0.078	0.062	1.391	0.282	0.046	–	0.108	0.044	1.354	0.025	0.153	0.318

References

Aitken, S. A., Colom, J. C., Henderson, C. M., & Johnston, P. A. (2002). Stratigraphy, paleoecology, and origin of Lower Devonian (Emsian) carbonate mud buildups, Hamar Laghdad, eastern Anti-Atlas, Morocco, Africa. *Bulletin of Canadian Petroleum Geology, 50*, 217–243.

Alexander, R. R. (1986). Resistance to and repair of shell breakage induced by Durophages in Late Ordovician brachiopods. *Journal of Paleontology, 60*, 273–285.

Balinski, A. (1971). *Stringocephalus burtini* Defrance from the environs of Siwierz, Poland. *Acta Paleontologica Polonica, 16*, 461–473.

Balinski, A. (1993). A recovery from sublethal damage to the shell of a Devonian spiriferoid brachiopod. *Acta Paleontologica Polonica, 38*, 111–118.

Balinski, A., & Biernat, G. (2003). New observations on rhynchonelloid brachiopod *Dzieduszyckia* from the Fammenian of Morocco. *Acta Palaeontologica Polonica, 48*, 463–474.

Bambach, R. K. (1999). Energetics in the global marine fauna: a connection between terrestrial diversification and change in the marine biosphere. *Geobios, 32*, 131–144.

Belka, Z. (1994). Dewońskie budowle weglanowe (Carbonate build-ups) Sahary Środkowej i ich związek z podmorskimi źródłami termalnymi (Carbonate mud buildups in the Devonian of the Central Sahara: evidences for submarine hydrothermal venting). *Przeglad Geologiczny, 5*, 341–346. [in Polish].

Belka, Z. (1998). Early Devonain Kess–Kess carbonate mud mounds of the eastern Anti-Atlas (Morocco), and their relation to submarine hydrothermal venting. *Journal of Sedimentary Research, 68*, 368–377.

Berkowski, B. (2006). Vent and mound rugose coral associations from the Middle Devonian of Hamar Laghdad (Anti-Atlas, Morocco). *Geobios, 39*, 155–170.

Berkowski, B., & Klug, C. (2012). Lucky rugose corals on crinoid stems—unusual examples of subepidermal epizoans from the Devonian of Hamar Laghdad (Morocco). *Lethaia, 45*, 24–33.

Bordeaux, Y. L., & Brett, C. E. (1990). Substrate specific associations of epibionts on Middle Devonian brachiopods: implication for paleoecology. *Historical Biology, 4*, 203–220.

Boucot, A. J. (1975). *Evolution and extinction rate controls* (pp. 426). New York, Elsevier.

Boucot, A. J., Johnson, J. G., & Struve, W. (1966). *Stringocephalus*, ontogeny and distribution. *Journal of Paleontology, 40*, 1349–1364.

Brachert, T., Buggisch, W., Flügel, E., Hüssner, H., Joachimski, M. M., & Tourneur, F. (1992). Controls of mud mound formation: the Early Devonian Kess–Kess carbonates of the Hamar Laghdad, Anti-Atlas, Morocco. *Geologische Rundschau, 81*, 15–44.

Brand, U., Logan, A., Hiller, N., & Richardson, J. (2003). Geochemistry of modern brachiopods: applications and implications for oceanography and paleoceanography. *Chemical Geology, 198*, 305–334.

Brett, C. E., & Walker, S. E. (2002). Predators and predation in Paleozoic marine environments. *Paleontological Society Papers, 8*, 93–118.

Brunton, C. H. C. (1966). Predation and shell damage in a Visean brachiopod fauna. *Palaeontology, 9*, 355–359.

Bultynck, P., & Walliser, O. H. (2000) Emsian to Middle Frasnian sections in the northern Tafilalt. *Notes et Mémoires du Service Géologique du Maroc*, *399*, 11–20.

Cavalazzi, B., Barbieri, R., & Ori, G. G. (2007). Chemosynthetic microbialites in the Devonian carbonate mounds of Hamar Laghdad (Anti-Atlas, Morocco). *Sedimentary Geology, 200*, 73–88.

Clausen, C.-D. & Leuteritz, K. (1984). Erläuterungen zu Blatt 4516 Warstein. *Geologische Karte von Nordrhein-Westfalen 1:25 000, Erläuterungen*, *4561*, 1–155.

De Baets, K., Klug, C., & Korn, D. (2011). Devonian pearls and ammonoid-endoparasite coevolution. *Acta Palaeontologica Polonica, 56*, 159–180.

Eggert, F. (2005). *Standardfreie Elektronenstrahl-Mikroanalyse* (pp. 1–187). Praxis: Ein Handbuch für die.

Elliott, D. K., & Bounds, S. D. (1987). Causes of damage to brachiopods from the Middle Pennsylvanian Naco formation, Central Arizona. *Lethaia, 20*, 327–335.

Elliott, D. K., & Brew, D. C. (1988). Cephalopod predation on a Desmoinesian brachiopod from the Naco formation, Central Arizona. *Journal of Paleontology, 62*, 145–147.

Franchi, F., Schemm-Gregory, M., & Klug, C. (2012). A new species of *Ivdelinia* Andronov, 1961 from the Moroccan Givetian and its palaeoecological and palaeobiogeographical implications. *Bulletin of Geosciences, 1*, 1–11.

Hallam, A. (1968). Morphology, palaeoecology and evolution of the genus *Gryphaea* in the British Lias. *Philosophical Transaction of the Royal Society, London, B, 254*, 91–128.

Hassan, F. (1978). Impurity-related centers in a pale green calcite crystal. *American Mineralogist, 63*, 732–736.

Hollard, H. (1974). Recherches sur la stratigraphie des formations du Dévonien moyen, de l'Emsien supérieur au Frasnien, dans le Sud du Tafilalt et dans le Ma'der (Anti-Atlas oriental). *Notes et Mémoires du Service Géologique du Maroc, 264*, 7–68.

Kaufmann, B. (1996). *Middle Devonian mud mounds of the Maïder Basin in the eastern Anti-Atlas, Morocco*. In G. Flajs, M. Vigener, H. Keupp, D. Meischener, F. Neuweiler, J. Paul, J. Reitner, K. Warnke, H. Weller, P. Dingle, C. Hensen, P. Schäfer, P. Gautret, R.R. Leinfelder, H. Hüssner & B. Kaufmann (Eds.), *Mud mounds: A polygenetic Spectrum of Fine-grained Carbonate Buildups*, volume 32 (pp. 49–57), Facies.

Kaufmann, B. (1997). Diagenesis of Middle Devonian carbonate mounds of the Mader Basin (eastern Anti-Atlas, Morocco). *Journal of Sedimentary Research, 67*, 945–956.

Kaufmann, B. (1998). Facies, stratigraphy and diagenesis of Middle Devonian reef- and mud-mounds in the Mader (eastern Anti-Atlas, Morocco). *Acta Geologica Polonica, 48*, 43–106.

Kaufmann, B., Schauer, M., & Reinhold, C. (1999). Concentric-zoned calcite cements of Middle Devonian carbonate mounds of the Mader Basin (eastern Anti-Atlas, Morocco)-a combined cathodoluminescence and microprobe study. *Neues Jahrbuch für Geologie und Paläontologie Abhandlungen, 214*, 95–110.

Klug, C. (2002). Quantitative stratigraphy and taxonomy of late Emsian and Eifelian ammonoids of the eastern Anti-Atlas (Morocco). *Courier Forschungsinstitut Senckenberg, 238*, 1–109. Frankfurt am Main.

Klug, C. (2007). Healed injuries on the shells of Early Devonian cephalopods from Morocco. *Acta Palaeontologica Polonica, 52*, 799–808.

Klug, C., Kröger, B., Kiessling, W., Mullins, G. L., Servais, T., Frýda, J., et al. (2010). The Devonian nekton revolution. *Lethaia, 43*, 465–477.

Klug, C., Schulz, H., & De Baets, K. (2009). Red trilobites with green eyes from the Early Devonian of the Tafilalt (Morocco). *Acta Palaeontologica Polonica, 54*, 117–123.

Kobluk, D. R., & Mapes, R. H. (1989). The fossil record, function, and possible origin of shell colour patterns in Paleozoic marine invertebrate. *Palaios, 4*, 63–85.

Lee, M. R., Torney, C., & Owen, A. W. (2007). Magnesium-rich intralensar structures in schizochroal trilobite eyes. *Palaeontology, 50*, 1031–1037.

Lee, M. R., Torney, C., & Owen, A. W. (2012). Biomineralisation in the Palaeozoic oceans: evidence for simultaneous crystallisation of high and low magnesium calcite by phacopine trilobites. *Chemical Geology, 314–317*, 33–44.

Massa, D., Combaz, A., & Manderscheid, G. (1965). Observations sur les séries Siluro-Dévoniennes des confins Algéro-Marocains du Sud. *Notes et Mémoires, Compagnie FranVaise des Pétroles, 8*, 1–187.

Nützel, A., & Frýda, J. (2003). Paleozoic plankton revolution: evidence from early gastropod ontogeny. *Geology, 31*, 829–831.

Richter-Bernburg, G. (1953). Zur Tektonik des mitteldevonischen Massenkalkes (Beobachtungen aus dem Gebiet von Warstein, Westfalen). *Zeitschrift der Deutschen Geologischen Gesellschaft, 104*, 94–98.

Roch, E. (1934). Sur des phénomènes remarquables observés dans la région d'Erfoud (confins algéro-marocains du Sud). *Association Études de la Géologie Méditerranéenne Occidentale, 5*, 1–10.

Sarycheva, T. G. (1949). The study of damage to carboniferous productoid shells. *Trudy Paleontologicheskiy Institut, 18*, 280–292. (in Russian).

Saunders, W. B., Spinosa, C., Teichert, C., & Banks, R. C. (1978). The jaw apparatus of recent *Nautilus* and its paleoecological significance. *Palaeontology, 21*, 129–141.

Signor, P. W, I. I. I., & Brett, C. E. (1984). The mid-Paleozoic precursor to the Mesozoic marine revolution. *Paleobiology, 10*, 229–245.

Slotta, F., Klug, C., & Keupp, H. (2011). Sublethal shell injuries in Late Devonian ammonoids (Cephalopoda) from Kattensiepen (Rhenish Mountains). *Neues Jahrbuch für Geologie und Paläontologie Abhandlungen, 261*, 321–336.

Swinehart, J. H., & Smith, K. W. (1979). Iron and manganese deposition in the periostraca of several bivalve molluscs. *Biological Bulletin, 156*, 369–381.

Töneböhn, R. (1991). Bildungsbedingungen epikontinentaler Cephalopodenkalke (Devon, SE-Marokko). *Göttinger Arbeiten zur Geologie und Paläontologie, 47*, 1–114.

Wendt, J. (1993). Steep-sided carbonate mud mounds in the Middle Devonian of the eastern Anti-Atlas, Morocco. *Geological Magazine, 130*, 69–83.